

N64-27910

FACILITY FORM 602

(ACCESSION NUMBER)

56

(PAGES)

CB-56511

(NASA CR OR TMX OR AD NUMBER)

(THRU)

1

(CODE)

15

(CATEGORY)

OTS PRICE

XEROX

\$

5.60 pp.

MICROFILM

\$

development

research

manufacture

components

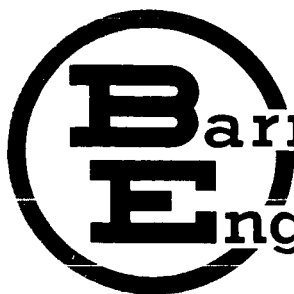
systems

instruments

BARNES ENGINEERING COMPANY

30 Commerce Road

Stamford, Connecticut



Barnes

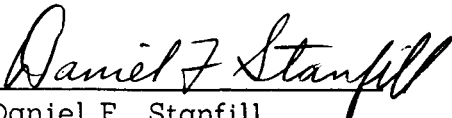
Engineering Company

30 Commerce Road • Stamford, Connecticut

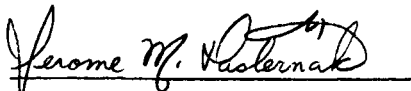
FINAL ENGINEERING REPORT
HORIZON SCANNER FOR VENUS AND MARS
BEC MODEL 13-170

Prepared For
Jet Propulsion Laboratory
Pasadena, California
JPL Contract 950016 under NASA-NAS7-100

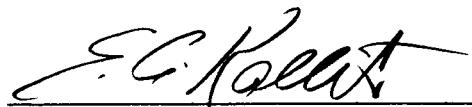
Prepared by:


Daniel F. Stanfill

Project Manager


Jerome M. Pasternak

Approved by:



Eli A. Kallet, Manager
Space Systems Department

TABLE OF CONTENTS

<u>Section</u>		<u>Page</u>
1.0	INTRODUCTION	1-1
	1.1 SCOPE	1-1
	1.2 APPLICABLE DOCUMENTS	1-1
	1.3 PROGRAM OBJECTIVES	1-1
	1.4 SUMMARY OF RESULTS	1-2
	1.5 NOMENCLATURE	1-3
2.0	SYSTEM DESCRIPTION	2-1
	2.2 PRINCIPLES OF OPERATION	2-1
	2.3 SCAN PATTERN	2-6
	2.4 SYSTEM SENSITIVITY	2-9
	2.5 SCAN MECHANISM	2-10
	2.6 SYSTEM OPTICS	2-11
	2.7 ELECTRONIC CIRCUIT DESCRIPTION	2-13
3.0	SCANNER CONSTRUCTION	3-1
	3.1 STRUCTURE	3-1
	3.2 TEMPERATURE CONTROL	3-1
	3.3 THE HERMETIC SEAL	3-4
	3.4 ASSEMBLY TECHNIQUE	3-5
	3.5 GEARS AND BEARINGS	3-6
	3.6 LUBRICATION	3-6
	3.7 SCAN AND ACQUISITION DRIVE MOTORS	3-7
	3.8 STRETCH CORDS	3-7
	3.9 THE USE OF BERYLLIUM IN SCANNER S/N 104	3-7
4.0	TEST EQUIPMENT, PROCEDURES AND RESULTS	4-1
	4.1 SIMULATION OF TARGETS	4-1
	4.2 TEST EQUIPMENT	4-3
	4.3 TEST PROCEDURES AND RESULTS	4-4
5.0	CONCLUSIONS AND RECOMMENDATIONS	5-1

APPENDIX A

HORIZON SCANNER MODEL 13-170 SCHEMATIC DIAGRAM

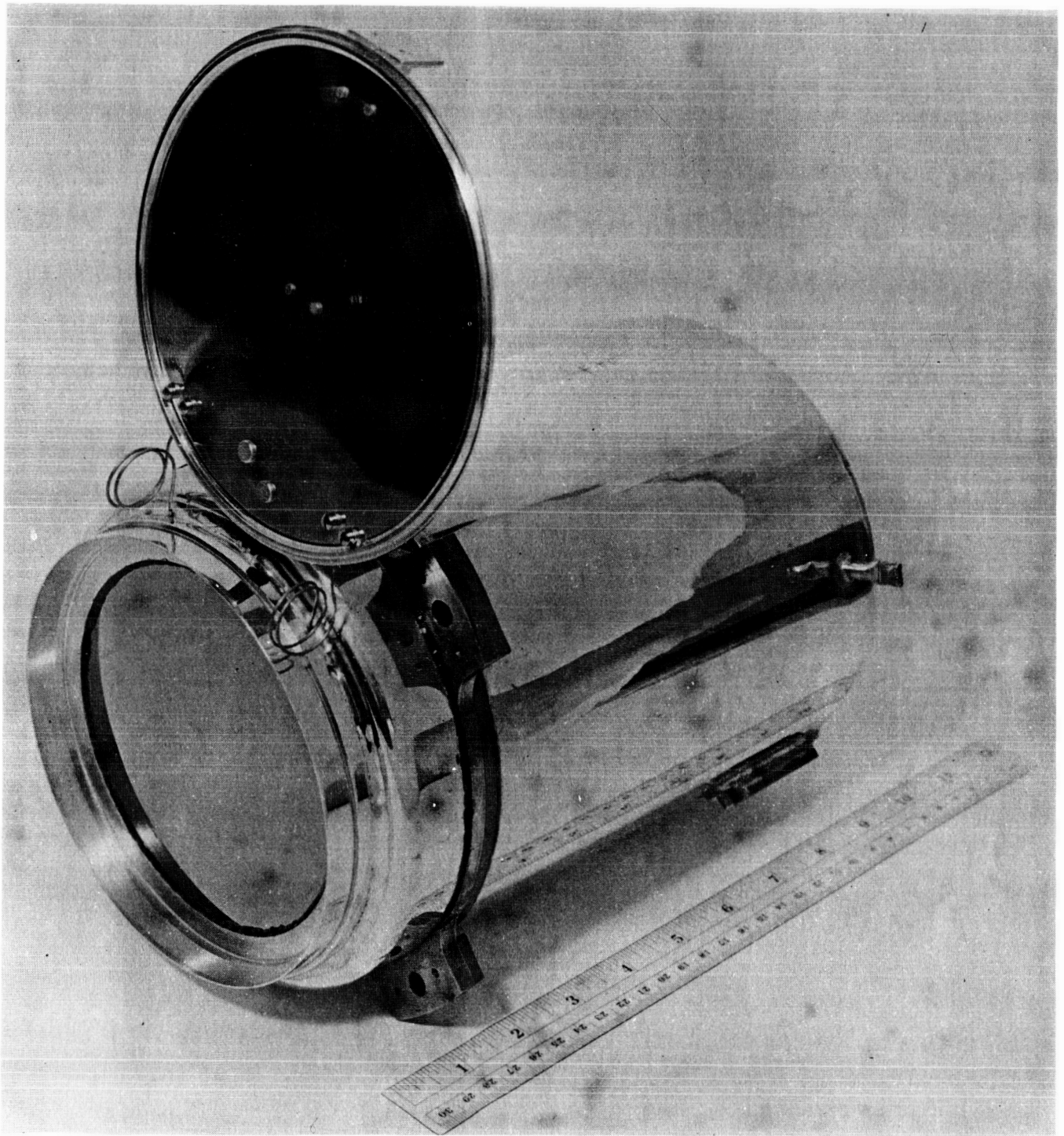


FIGURE 1-1 INFRARED HORIZON SCANNER, MODEL 13-170

Section 1.0 INTRODUCTION1.1 SCOPE

This engineering report is principally concerned with the design and performance of Model 13-170 Infrared Horizon Scanner, developed for use on fly-by planetary probes to Mars and Venus. Fabrication, assembly and test fixtures are also discussed. The report was prepared in accordance with the requirements of JPL Contract 950016, Statement of Work SW1600, Article 1, Paragraph (2) (4), which states:

"Barnes Engineering Company shall submit a final engineering report covering the design, fabrication, assembly and functional test procedure of the Horizon Scanner Flight Prototype Units and Horizon Scanner Test Fixture."

1.2 APPLICABLE DOCUMENTS

- a. JPL Contract 950016
- b. JPL Statement of Work SW1600
- c. JPL Spec. 30374 Spacecraft Design Specification
Mariner A Flight Equipment, Horizon
Scanner for Attitude Control
- d. JPL Spec. 30856A Test Specification, Mariner B
Flight Equipment, Attitude Control Subsystem,
Horizon Scanner Assembly (7A16)
- e. JPL Drawing No. D4800734 Horizon Scanner Assembly,
Mars Configuration, Control Drawing
- f. BEC Proposal No. P323
Proposal for Horizon Sensor for Venus Probe
- g. BEC Drawing No. R4253-001
- h. Test Report
Delrin Gear Life Test for Venus and Mars Horizon Sensor
- i. Study Report BEC-4253-R22A
Non-Magnetic Structural Materials for
Venus and Mars Horizon Sensor
- j. U.S. Patent No. 3,083,611 Multi-Lobar Scan Horizon Sensor

1.3 PROGRAM OBJECTIVES

The objectives of this program, as delineated in the Statement of Work SW1600, was to design, develop and construct an infrared horizon scanner

capable of locating and tracking targets subtending 2.4° through 52° , i.e., planet Mars at 100,000 miles range and Venus at 5000 miles, respectively.

The scanner was to produce d-c error signals representing the target displacement from the instrument optical axis in a two-axis coordinate system with an accuracy of one sigma of $\pm 0.1^\circ$. The d-c volt signals were to be proportional for target displacement up to $\pm 1/3$ of a degree. The instrument operation was to include an initial search mode capable of acquiring a target lying 8° off the scanner optical axis and an automatic switchover to tracking mode of operation.

The scanner was to be so constructed as to withstand launch and deep space stresses and environments, limitations of 10 pounds total weight per system and 10 watts maximum power consumption were specified.

1.4 SUMMARY OF RESULTS

The accuracy of the Horizon Scanner when using an ideal test target, exceeds the design objective of establishing local vertical in two axes to an accuracy of one sigma of $\pm 0.1^\circ$. However, certain errors, such as the terminator on Mars, and the sun lying near the scan path, will create errors which exceed the 0.1° accuracy requirement (see Sources of Error).

The Horizon Scanner successfully withstood vibration, shock and temperature tests in accordance with JPL Spec. 30257 without deterioration of performance. In the final configuration, the weight requirement of 10 pounds was exceeded by 2-1/2 pounds, while total power consumption remained within the 10 watt limit.

1.4.1 System Specifications

Size:	6-1/2" dia. x 9-1/2" long
Weight:	12.5 pounds
Power:	50v rms, 2400 cycle square wave, 5 watts; 26v 400 cps: 3-1/2 watts (tracking), 5 watts peak (acquisition)
Accuracy:	$\pm 0.1^\circ$, one sigma, each axis
Output:	600 mv d-c per 0.1° , linear to $\pm 1.3^\circ$, saturating at ± 2 volts
Output Bandwidth:	1/6 cps
Signal/Noise at 230°K:	700/1
Optical Material:	Germanium

Spectral Response: $1.8\mu - 22\mu$
Optical Filter: None
Effective Aperture: 3" dia.
f/number: f/0.23

1.5 NOMENCLATURE

Throughout this report, reference is made to "hinge" and "swivel". These designations are derived from the possible two degrees of freedom motion of the spacecraft auxiliary platform, and is to be distinguished from the pitch, roll and yaw axes of the spacecraft.

The hinge and swivel error outputs of the Horizon Scanner are the control signals by which the auxiliary platform is kept aligned with the local vertical by a rotation about the hinge and swivel axes. The two axes are correlated with the three mounting pads (or "ears") of the Horizon Scanner. The hinge axis is parallel to the line which passes through the two diametrically opposite mounting pads. Swivel axis is parallel to the line which passes through the central mounting pad, and is perpendicular to hinge axis. Furthermore, the optical axis or boresight of the instrument, forms the third axis of the mutually perpendicular coordinate system.

Section 2.0 SYSTEM DESCRIPTION

Model 13-170 Infrared Horizon Scanner was designed primarily for use in the Mariner Spacecraft for Venus/Mars fly-bys. When installed in this vehicle, the scanner is used to orient the Mariner payload so that the basic measurement instruments may be kept directed at the planets. In this application, the scanner package is activated when the range from the planet is 100,000 miles and continues to operate to within 5000 miles of the planet. The scanner produces two axis error signals and is capable of locating and tracking a target as small as 2.4° (i.e., Mars at 100,000 miles) and give accurate attitude information for a target as large as 52° (Venus at 5000 miles).

During its flight, the Mariner Spacecraft is aligned so that the longitudinal axis of the vehicle lies along the sun line. The scanner is mounted upon a secondary boom which is extended from the vehicle during its flight in accordance with a pre-programmed schedule. In order for the sensor to acquire a target, it is mandatory for previous guidance and attitude controls to have oriented the Mariner Spacecraft so that the target planet falls within the overall view-angle of the scanning pattern. When a d-c error voltage appears at either output, step motors mounted on the vehicle drive the auxiliary boom or platform until null position is again restored. This closes the control loop, and allows the Horizon Scanner to act as a tracking device, at all times pointing toward the center of the planet.

The Horizon Scanner was designed to seek center of planets varying in view angle from 2.4° to 52° , to an accuracy one sigma of $\pm 0.1^\circ$. The overall transfer function of the Horizon Scanner is 6 volts d-c per degree, linear over ± 3 degrees and saturating at 2 volts. Testing has demonstrated tracking accuracy of 2 to 3 minutes, repeatability and angular threshold also falling within this band.

2.2 PRINCIPLES OF OPERATION

All objects whose temperature is greater than absolute zero emit infrared energy. The planets Venus and Mars, when viewed by an infrared scanner of wide bandwidth (in this case 1.8μ to 22μ), appear as blackbody emitters of approximately 235°K . Compared with deep space, whose blackbody temperature is no more than 11°K , the planets appear, to an infrared detector, as a bright, luminous object against a dark background. The presence of this thermal discontinuity within the system scan pattern is used to derive platform attitude information and to generate error signals.

The instantaneous field of view of the scanner is $1/2^\circ \times 1/2^\circ$ and it is swept through a four leaf rosette pattern. The four extremities of the rosette (i.e., the leaf tips) define a 70° conical view angle of the system, see Figure 2-1. For each sweep across a planet, the scanner detects the change in irradiance level at two horizon points. The scan pattern is generated by two counter-rotating

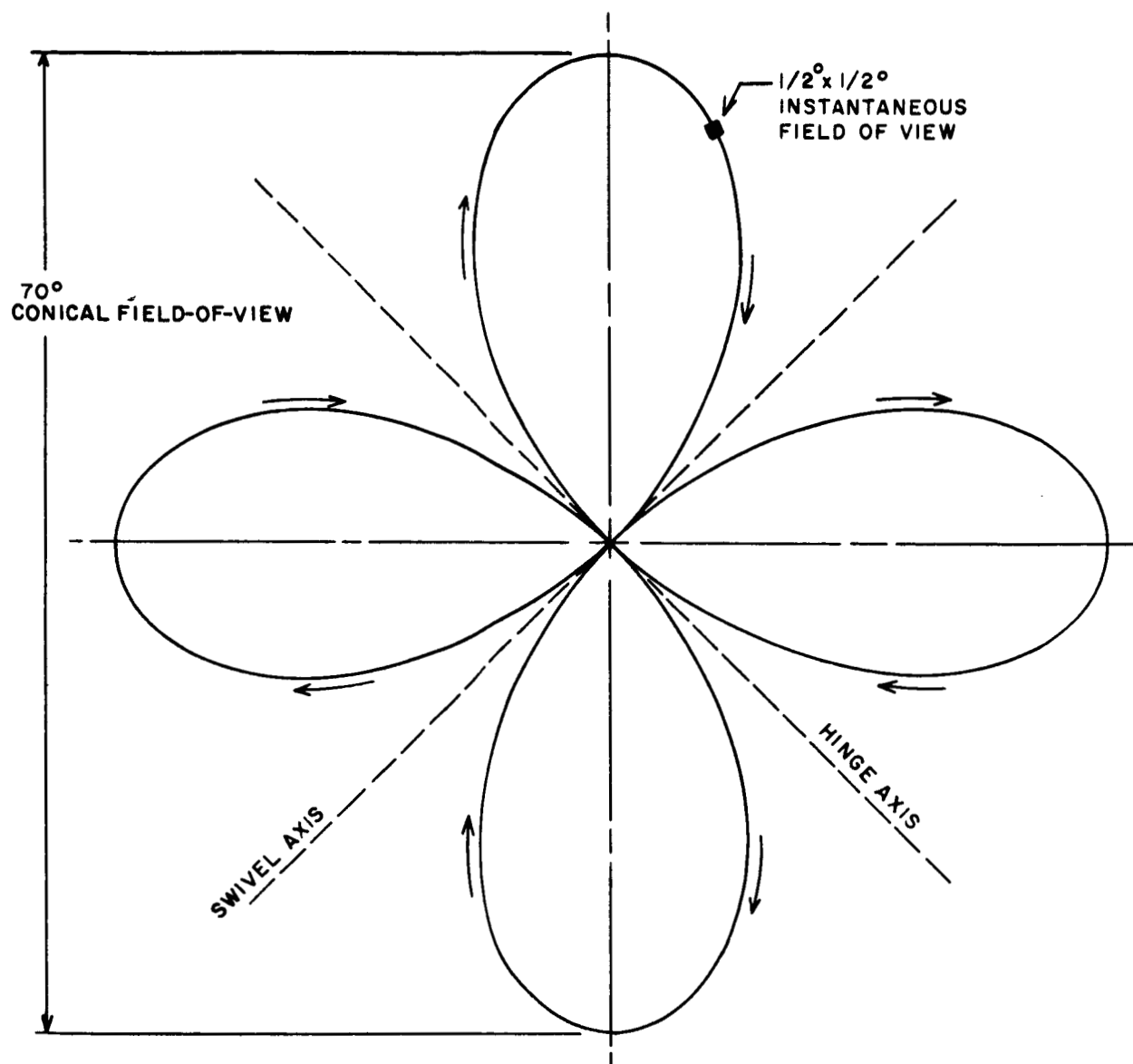


Figure 2-1 SCAN PATTERN AND ORTHOGONAL AXES

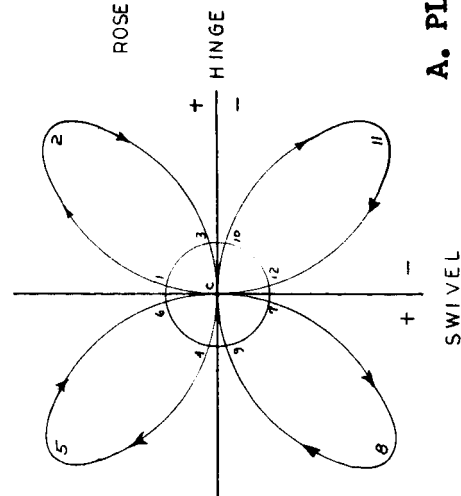
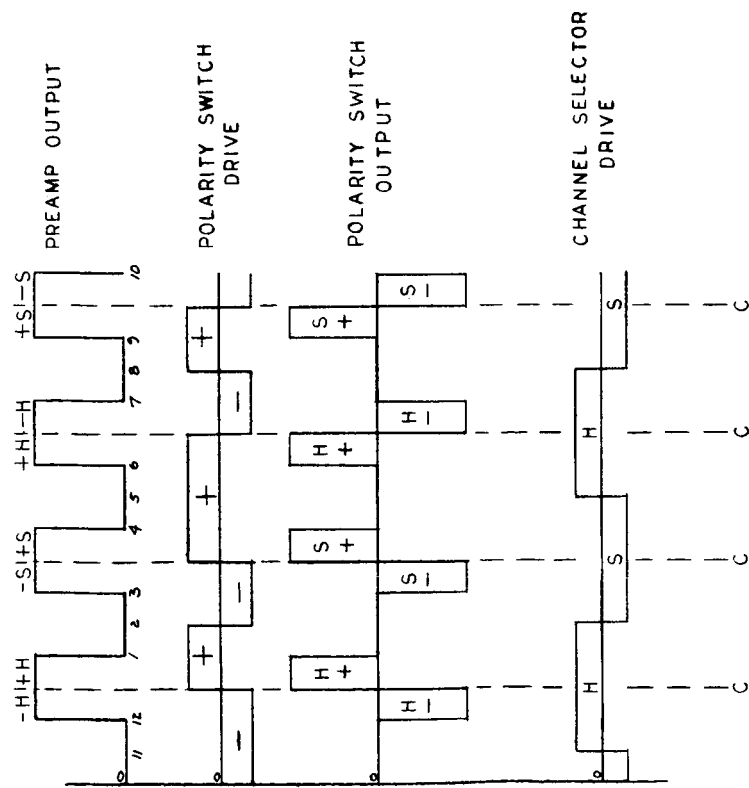
germanium prisms operating with a speed ratio of 3:1. The largest possible detector area will give the best sensitivity. However, experience has shown that an instantaneous field of view of $1/2^\circ \times 1/2^\circ$ is a good compromise to best yield the 0.1° horizon accuracy, considering the angular subtense of the planets involved. The system therefore has a 3-inch diameter aperture with a $3/4$ -inch focal length ($f/0.23$) and a thermistor detector size subtending $1/2^\circ \times 1/2^\circ$. The optical dimensions of the sensitive flake should therefore be 0.6×0.6 mm which by the use of the germanium immersed lens was reduced by a factor of 4 to 0.15×0.15 mm.

The scan speed has been chosen to give an ample sampling rate and yet not exceed the time constant limitations of the detector. A thermistor detector having a time constant of 1 millisecond is used. Therefore, a scanning rate such as to generate seven lobes per second was selected to cause the $1/2^\circ$ detector to cross the horizon in 1 millisecond. To generate this pattern, one prism must rotate at a speed of 315 rpm and the second at 105 rpm in the opposite direction. These speeds do not place undue demands on the motor or bearings.

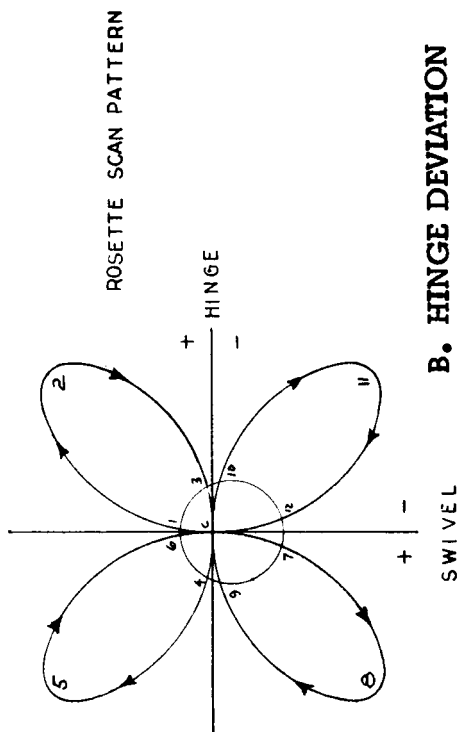
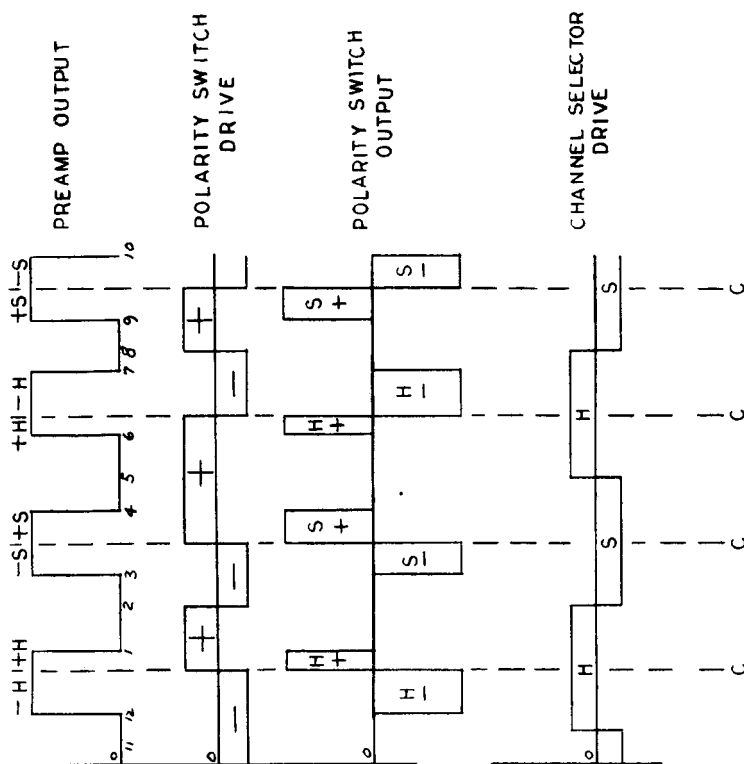
For acquisition purposes, a second drive motor rotates the entire counter-rotating prism assembly. Acquisition search mode only requires that this assembly rotate through a maximum angle of 90° at a rate of no more than $1/4$ rpm. When the pattern is rotated, it is necessary to locate the hinge and swivel axes of the scan pattern with reference to the axes of the platform itself. For this purpose a synchro resolver is connected to the rotating piece to readout the necessary angular information. It is important to realize here that only the prism optical-mechanical assembly is rotated and not the detector.

The system electronics, then compares the time interval between the two horizon crossovers with a fixed reference. It also compares pulse width of alternate sweeps, see Figure 2-2. From these bits of information, the scanner generates error signals corresponding to the direction of tilt between the conical scan axis and the local vertical. As the instantaneous field of view scans across the thermal discontinuity, a signal pulse is generated by the infrared detector. Successive crossovers produce a train of such pulses. In addition, two reference pulses are generated internally, one when the field coincides with the rosette center, and another at each extreme of the scan. These reference pulses are generated by a reference wheel, mounted on a slow speed prism, which interrupts two lamp-photodiode pairs, see Figure 2-3.

Signal processing is based on pulse centering techniques. Raw pulses from the detector are preamplified and then limited, resulting in a train of rectangular pulses whose amplitude is independent of planet radiance. Pulses alternately representing hinge and swivel, are derived from vertical and horizontal sweeps of the rosette. Since hinge and swivel pulses occur alternately in time, the data is time shared through the electronics until channel separation is required. Following separation, the signals are chopped, amplified and fed to a synchro



A. PLANTET



B. HINGE DEVIATION

FIGURE 2-2 PREAMPLIFIER OUTPUT GATING

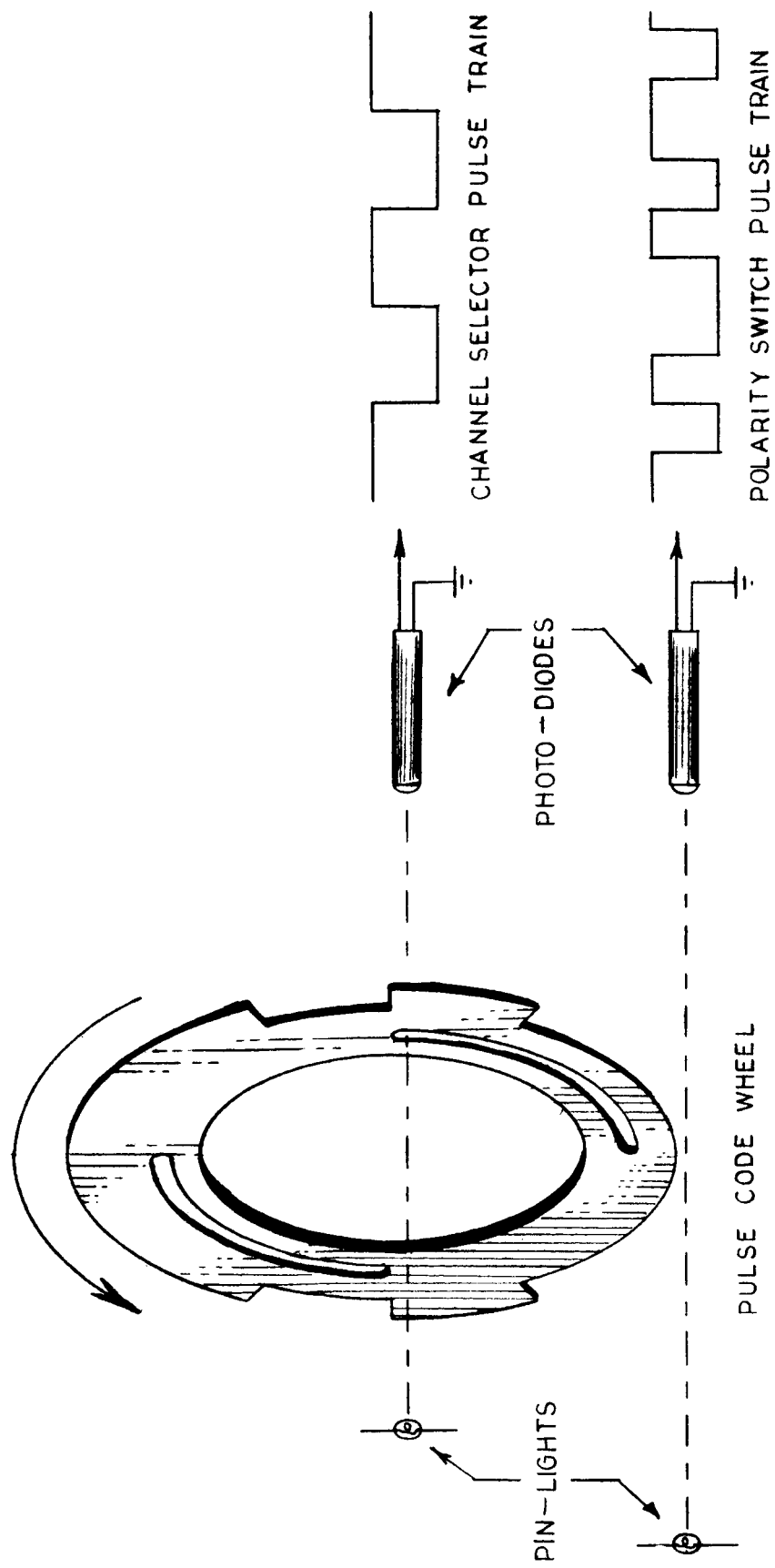


FIGURE 2-3 PULSE GENERATOR

resolver which is used to correlate scanner axes to platform axes. The resolved a-c signal is demodulated and yields the desired d-c output.

After every forward sweep across the planet face, a back sweep is alternately generated by the rosette. Therefore, alternate pulses within a channel must be sequence inverted to properly sort the information. This is done by inverting the front half of a signal pulse, and then the rear half of the succeeding alternate pulse. Thus, the plus and minus d-c level generated is truly indicative of axis error.

When the planet is centered within the rosette pattern, a sync pulse (denoting optical center) coincides with the center of the signal pulse, and no output appears at either channel. This null condition indicates that the optical axis, or boresight, of the instrument coincides with local vertical. Any phase shift, or decentering, of the signal pulse with respect to the sync pulse creates a d-c voltage whose polarity indicates the error direction. This d-c error signal, after further processing, becomes the output signal from each channel.

To achieve a d-c voltage proportional to the phase shift of the signal pulse, the pulse is limited and the initial portion is fed to a capacitor integrator. The integrator continues charging until the sync pulse, operating a solid state switch, applies signal of inverted polarity, and begins discharging the integrator during the residual portion of the signal pulse. If the pulse width before sync is identical to pulse width after sync, no net charge remains in the integrator. If the pulse widths occurring before and after sync are not equal, a net charge will remain in the integrator. The polarity of this charge indicates the direction of signal error, and is proportional to target displacement over a finite range.

2.3 SCAN PATTERN

After giving consideration to a number of possible scanning methods, the four leaf rosette was chosen because it offers several advantages for a fly-by mission. During encounter, target size changes drastically, appearing small at large distances and becoming progressively larger as the spacecraft nears the planet. A rosette scan is able to cope, simply and directly, with this problem of changing geometry.

The need for two-axis information derived from a single scanning head, leads to a choice of a rosette having four leaves as orthogonal information is directly available from such a scan pattern.

From the standpoint of information theory, the rosette is highly efficient; during a complete scan the instantaneous field of $1/2^\circ \times 1/2^\circ$ need sample only 4.3% of the total 70° view angle, providing a high sample rate.

An important bonus of the four leaf rosette scan is error cancellation. Because successive samples cross over the target in opposite directions,

several types of fundamental errors, such as unequal horizon temperatures, are cancelled; (for a more complete discussion, see Sources of Error).

Finally, the four leaf rosette scan offers the advantage of eight horizon samples per complete scan, which tend to average the effect of horizon temperature abnormalities, terrain unevenness, etc. The planet is thus bracketed within the eight sample arrays to a higher accuracy than that possible by direct line scanning in two axes (which would provide only four horizon samples per scan).

The two orthogonal axes, hinge and swivel, are established within the scan pattern as shown in Figure 2-1. These axes relate to the two motions, or axes of the spacecraft auxiliary platform, and provide the spacial coordinates by which the planet is tracked.

2.3.1 Acquisition

Since the rosette scan samples only a small percent of the conical view angle, small subtense planets must be acquired by one or more sweeps of the rosette before tracking begins. A signal presence circuit is used to activate the acquisition or search mode if a useable signal is not detected by the scanner. A small motor rotates the rosette pattern at 1/4 rpm through 90°, thereby sweeping the entire conical view angle. Limit switches reverse the sweep of the rosette at each end of the 90° sector. This mode continues until a useable signal is detected by the scanner. The signal presence circuit then turns off the acquisition motor. Any subsequent loss of signal causes reactivation of the acquisition mode.

As the rosette scan pattern oscillates back and forth through the 90° sector search, the hinge and swivel coordinates also become rotated. A synchro resolver is used to transform the rotated coordinates back to the fixed reference coordinates of the spacecraft auxiliary platform.

2.3.2 Sources of Error

2.3.2.1 Sun Near Scan - When the sun lies near the scan path, a real image is formed in the focal plane of the detector. This sun image may be sufficiently close to the thermistor detector flake to cause local heating of the germanium, resulting in a false signal. This effect begins to occur when the scan passes within 6° to 8° of the sun. This signal will be sufficiently strong to enter the slicing level, and will cause an error by injecting false signal into the integrator. This will displace the apparent local vertical toward the direction of the false signal, and produces a fundamental system error. (See Recommendation 3 in Section 5.0.)

2.3.2.2 Mars Terminator - If the scanner had an infinitely fast response, the Mars terminator would not cause error. Since, however, the real response at

the output of the preamplifier is approximately 2 milliseconds, the terminator leads to a fundamental error.

Consider a single time constant device scanning across a uniform temperature target. The leading and trailing edges of the pulse will be an exponential rise and decay. If a slicing level of 50% is used, the delay time will be equal at both leading and trailing edges. Since the rosette pattern alternately reverses the direction of crossover, the net effect will be zero, since the pulse shift error induced by one crossover is cancelled by the succeeding crossover.

Carrying the argument further, any slicing level will produce zero total error when used with the rosette scan, since there is always a net cancellation from succeeding scans. If, however, the leading and trailing edges are of unequal magnitude, the error cancellation no longer holds true. This is the situation with the Mars terminator, where the sunlit side may appear to be 300°K, and the dark side only 200°K. Considering spectral efficiencies, the warm side produces a signal 6.2 times the magnitude of the cold side. When the slicing is maintained at a low level, in order not to miss the cold edge, pulse shift error is not cancelled, and a fundamental offset results. Thus, assuming the terminator produces a 6.2:1 variation in signal level, a fundamental error shift up to 0.4° toward the warm side may be experienced. Since mission geometry may be predicted in advance, this error may be compensated by computer programming, or in other ways.

2.4 SYSTEM SENSITIVITY

The system sensitivity may be evaluated from a knowledge of the radiance levels to be detected and a calculation of the system noise equivalent power (NEP).

Venus has been measured, in the 8 to 13 micron region, to have a mean temperature of 234°K. The temperature of Mars varies from 200°K at 0700 local Mars time to 300°K at 1200*. If we assume 0°K for outer space and 200°K for the planet for safety, this amounts to a total blackbody radiance of 0.003 watts/cm²/steradian. Some of this, however, will be lost due to the variation of spectral transmission of germanium. Germanium transmission begins to decline at 15 microns and falls nearly to 0 at 30 microns before rising again. This results in a loss of approximately 40% of the energy leaving, approximately 0.002 watts/cm²/steradian.

The noise equivalent power of a thermistor detector is given as:

$$NEP = 2(10^{-10}) \sqrt{\frac{A \Delta f}{T}}$$

* W. M. Sinton and John Strong, Astrophys. J. 131, March (1960).

where A = detector area in cm^2
 τ = detector time constant in sec.
 Δf = noise bandwidth in cps

The detector size for a $1/2^\circ \times 1/2^\circ$ field using a 3-inch focal length lens is 0.6×0.6 mm. The germanium immersion lens reduces this by a factor of 4 to 0.15×0.15 mm or $2.25 \times 10^{-4} \text{ cm}^2$.

The scan speed has been arranged to require approximately 1 msec. for the detector to cross the horizon resulting in a scan speed giving seven lobes/sec. Therefore, the detector time constant has been chosen as 1 msec.

The preamplifier bandwidth must be sufficient to pass the 7-cycle square wave pulses generated as the pattern crosses the planet, however, this is not the limiting noise bandwidth. The maximum frequency response of the output error signal can be as low as 1 cps. Therefore,

$$\begin{aligned} \text{NEP} &= 2(10^{-10}) \sqrt{2.25(10)^{-4} \times \frac{1}{.001}} \\ &= 0.95 \times 10^{-10} \text{ watts.} \end{aligned}$$

The system signal-to-noise ratio is given by

$$S/N = \eta_o \eta_e \frac{A_o H}{\text{NEP}}$$

where H = radiation density at aperture
 A_o = area of aperture
 η_o = optical efficiency
 η_e = electronic efficiency

The transmission of the germanium optics with anti-reflection coating will be about 0.35. The electronic efficiency would be unity if the system were limited by Johnson noise of the detector, but the input transistor's current noise reduces this by a factor of 4 giving an efficiency of 0.25.

The radiation density at the aperture is given by:

$$H = N\omega$$

where N = radiance difference
 $= 0.002 \text{ watts/cm}^2/\text{steradian}$
 ω = field of view
 $= 1/2^\circ \times 1/2^\circ = 64 \times 10^{-6} \text{ steradians}$
 $H = (0.002)(64(10)^{-6}) = 1.3 \times 10^{-7} \text{ watts/cm}^2$

The area of the aperture is 46 cm². Thus,

$$\begin{aligned} S/N &= \frac{(0.35)(0.25)(46)(1.3 \times 10^{-7})}{0.95 \times 10^{-10}} \\ &= 5500 \end{aligned}$$

This is the peak signal referred to rms noise. We can assume signals must be five times rms noise for reliable detection. This then gives a ratio of 1100:1. We can convert this to an angular error equivalent to noise. The peak signal will occur for the maximum error, which for the largest planet size will be 52°/2 or 26°. Therefore, the minimum reliability angular error will be equivalent to $\frac{26^\circ}{1100} = 0.024^\circ$.

2.5 SCAN MECHANISM

The sensor scan pattern is generated by two counter-rotating prisms gear driven by a 400 cycle, size 11, induction motor developed for the application. The two prisms, driven at a relative speed ratio of 3:1 (or a relative ω of 4:1), generate the four leaf rosette scan. Each germanium prism has a wedge angle of 5°25' and a refractive index of 4. The radiation is deflected 17-1/2° through each prism, resulting in a total of 35° off-axis deflection through the prism pair. Therefore, total view angle subtended by the rosette, measured from tip to tip, is 70 degrees.

The slow speed, or front, prism rotates at 105 rpm; the fast, or rear, prism rotates at 315 rpm. These speeds were chosen to be consistent with the detector response time of 1 millisecond. At the optical axis, the scan (tangential velocity) sweeps through 770 field degrees per second. Theoretical horizon crossover time for the 1/2° instantaneous field is a ramp function of 650 microseconds duration.

At the leaf tips of the rosette, tangential sweep velocity is 385 field degrees per second, half the velocity at center. Velocity variations are a property characteristic of this type of scan: instantaneous velocity being a transcendental function superimposed on a constant (or average) velocity. (For a complete derivation, refer to Appendix A.) This velocity variation does not cause any system error or variation, but does complicate the altitude output, which is a direct voltage analog of target pulse width.

A reference wheel, mounted on the slow speed prism, interrupts two pairs of lamps and photodiodes to generate switching and synchronizing information. The two lamp-photodiode pairs function on two separate tracks on the reference wheel. The inner track is alternately 90° on and 90° off, and drives two synchro-verter switches to sort pulses alternately into the hinge and swivel channels. The outer track has appropriate cut-outs to perform necessary signal inversions used to examine the d-c content occurring before and after rosette center crossover.

In the search mode of operation, the rosette scan pattern is rotated through a 90° sector search. Redundant microswitches are used as electrical limit stops, and cause reversal of direction at each end of the 90° sector. This oscillating search continues, at a rate of 90° per minute ($1/4$ rpm) until a target is acquired.

The rate of rotation of the acquisition drive is so chosen as to produce full coverage with minimum overlap. At the edge of the conical view angle, 35° off optical axis, the scan pattern is advanced one-half degree for each complete rosette pattern (four lobes). The instantaneous field of view, $1/2^\circ \times 1/2^\circ$, thus falls adjacent to the position it previously scanned during the previous cycle. This condition of no overlap holds true only at the edge of the conical view angle. Overlap is unavoidable elsewhere in the view angle, becoming progressively greater toward center. At the exact center, there is total and continuous overlap.

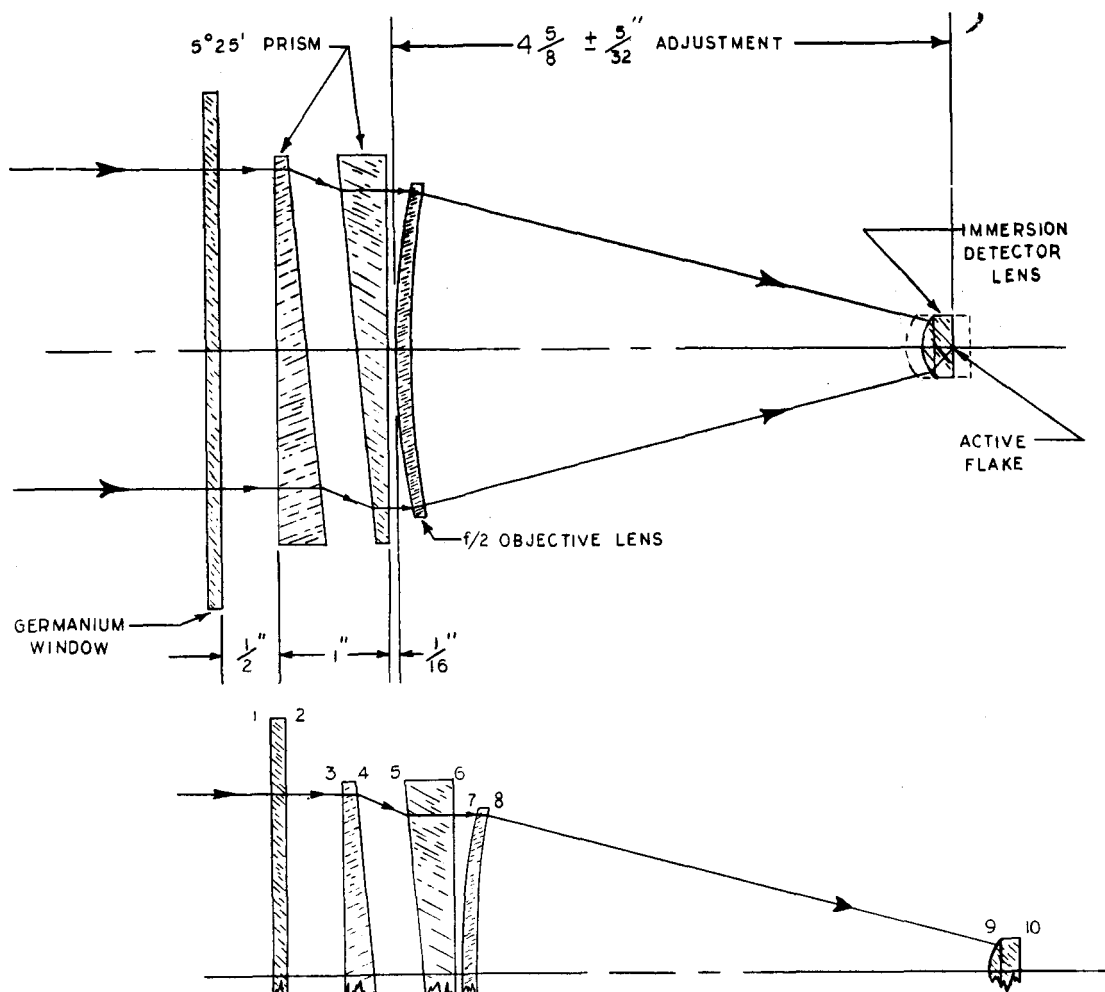
The entire mechanical scanning section, containing the two prisms, synchronizing wheel, photodiodes, and miniature lamps is rotated within a large $5\text{-}1/2$ inch I.D. bearing contained in the outer shell of the instrument. In this way, there is no differential motion between prisms, and the sync pulses are kept in proper relation to the scan pattern.

2.6 SYSTEM OPTICS

Target radiation passes through a three-inch aperture and is focused onto the detector surface by a germanium fabricated optical system. The two $5^\circ 25'$ prisms are mounted behind the germanium window, followed by an $f/2$ objective lens. A hyperhemisphere is used as the immersion element of the thermistor bolometer detector, and is used to correct objective lens aberration. This arrangement is shown in Figure 2-4.

The optics are coated with ZnS for $1/4\lambda$ at 12.5 microns and are optimized to receive radiation from planets having temperatures of about $235^\circ K$. The nine surface optical system has a peak efficiency of 35%; total efficiency of transmission over the spectral region has been calculated at 20%. In air, the optics would be equivalent to an $f/0.8$ system, but germanium immersion increases the speed by a factor of approximately 3.5, giving an $f/0.23$ system. The germanium system functions with no limiting filters. In the spectral region of interest, the index of refraction of germanium is essentially constant; chromatic aberration, therefore, is negligible.

Although a 0.4 milliradian diffraction limit is obtainable with a 6-inch spacing between objective and detector lenses, the system was compromised to 1.7 milliradians aberration by using shorter spacing to decrease overall size of the sensor. Aberration not exceeding $1/4$ the physical size of the sensitive thermistor flake is not detrimental to system performance.



SURF.	RADIUS & TOL.	CLEAR APERTURE	THICKNESS & TOL.	MATERIAL	$\lambda = 12.5$ INDEX	WEDGE TOL.	FIG. TOL.	SURF. CODE	SURF.
1	∞ "	4.750"	0.156 \pm 0.005"	OPTICAL GERMANIUM	4.002	0.002" T.I.R.	15 FRINGES	80 - 50	1
2	∞	4.750	≈ 0.500	AIR	1.000	—	15 FRINGES	80 - 50	2
3	∞	3.530	0.18 - 0.463 \pm 0.005	OPT. Ge	4.002	—	10	80 - 50	3
4	∞	3.530	0.074 - 0.419 \pm 0.010	AIR	1.000	—	10	80 - 50	4
5	∞	3.530	0.18 - 0.463 \pm 0.005	OPT. Ge	4.002	—	10	80 - 50	5
6	∞	3.530	≈ 0.0625	AIR	1.000	—	10	80 - 50	6
7	5.319 \pm 0.025	3.000	0.180 \pm 0.005	OPT. Ge	4.002	0.002 T.I.R.	10	80 - 50	7
8	7.749 \pm 0.050	2.960	4.475 \pm 0.150*	AIR	1.000	—	10	80 - 50	8
9	0.325 \pm 0.002	0.425	0.378 \pm 0.001	OPT. Ge	4.002	—	10	80 - 50	9
10	∞	0.050**					10	80 - 50	10

COATING: $\frac{1}{4}\lambda$ ZnS @ 12.5 μ ON SURF. 1 THRU 9

REMARKS : * FOCUSING ADJUSTMENT

** 0.15 X 0.15 mm THERMISTOR
CENTERED ON THIS SURF

FIGURE 2-4 OPTICAL SYSTEM

2.7 ELECTRONIC CIRCUIT DESCRIPTION (See Figure 2-5)

2.7.1 General

2.7.1.1 Thermistor Bolometer Detector - The infrared detector is a Barnes immersed thermistor bolometer, specially designed for this application. Flake size is 0.15 mm by 0.15 mm, time constant is 1 millisecond, and resistance per flake is 400K ohms. Responsivity is 500 volts per watt, when biased at 20 volts per flake.

2.7.1.2 Preamplifier - Five transistors are incorporated into this low noise, low frequency amplifier of bandwidth 0.1 to 700 cps. Overall feedback is used to stabilize the gain at 4400. The input impedance to this circuit is approximately 1.5 meg ohms. The junction of the thermistor flakes of the bolometer is a-c coupled to the input of this circuit so that the low level signals sensed by the detector may be amplified to a level suitable for processing.

2.7.1.3 Solar Presence - In order to prevent the preamplifier from being driven into prolonged saturation by a relatively strong sun signal appearing in the sensor's field of view, the Solar Presence circuit drives the preamplifier into negative saturation (from which it can quickly recover), whenever a signal about 80 times the maximum expected planet signal level is detected.

2.7.1.4 Fixed Slicing Level - Amplifier Clipper - The preamplifier is fed to a fixed slicing level circuit. This circuit is designed to start to turn on at a pre-set voltage level of the preamplifier output, and is completely turned on within 100 millivolts rise above the set level. The range of control is from 0.5v to 1.5v, corresponding to planet temperatures between 140°K and 190°K. The firing level selected depends on target characteristics, and is set by a potentiometer.

Because the information processing depends upon position of the normalized incoming signal pulse, the fixed slicing level is limited, or clipped, to yield a constant amplitude of $\pm 6v$.

2.7.1.5 Positive and Negative Clamp and Polarity Switch - The output of the clipper is channeled to two parallel signal paths. One path clamps the signal negatively at -12v, and the other inverts the incoming signal and clamps it positively at +12v. The signals are clipped to -6.3v and +6.3v respectively and then fed to two sides of a "single pole, double throw" solid state switch which is gated by the Polarity Switch Drive circuit. Output is taken from the center of the switch and fed to the channel selector and integrator circuit.

2.7.1.6 Channel Selector and Integrator - The output of the Polarity Switch, which consists of time-shared information, is fed into a symmetrical switching circuit gated by the Channel Selector Drive, for separation into two channel outputs. Each channel is then fed into separate integrating networks where the leading and trailing portions of the planet sweeps are compared. Any voltage

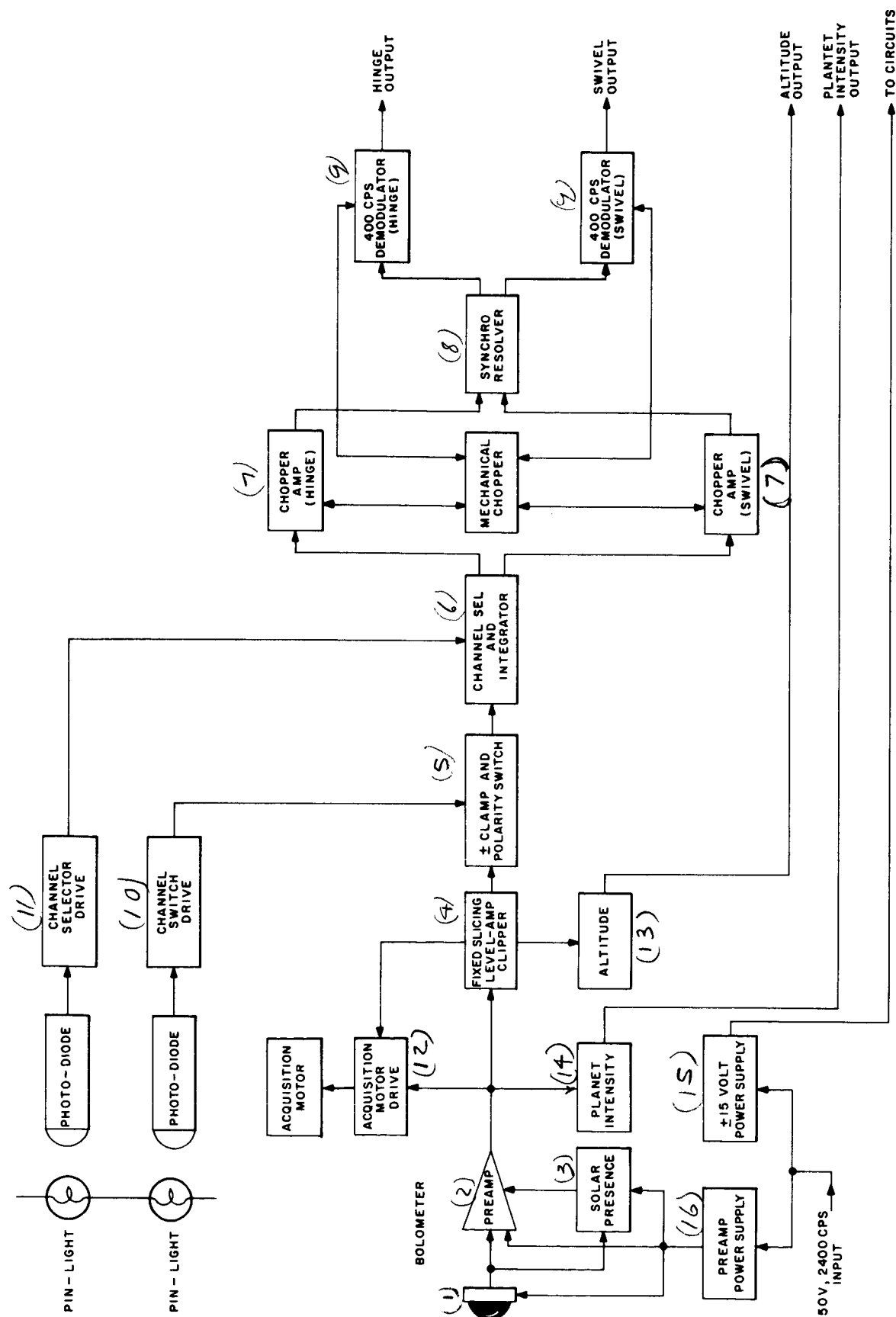


Figure 2-5 SYSTEM ELECTRONICS BLOCK DIAGRAM

20967

residue after adding oppositely polarized pulse widths will remain as a net charge on the output capacitor of the integrator.

2.7.1.7 Chopper Amplifier - D-C residue present at the output of either integrator circuits is chopped at a 400 cps rate and fed into an a-c amplifier of gain 300. The outputs of the chopper amplifiers, one for each channel, are fed to the two rotor windings of a synchro resolver.

2.7.1.8 Synchro Resolver - The synchro resolver performs a coordinate transformation. The search or acquisition mode, which oscillates the rosette pattern within a 90° sector, may acquire and stop at any arbitrary orientation. The synchro resolver shaft is geared 1 to 1 with respect to the rosette pattern axes, and thus correlates the error signals with respect to the hinge and swivel axes of the platform.

2.7.1.9 400 CPS Demodulator - The two channel, 400 cps demodulator receives signal from the stator windings of the resolver and performs synchronous demodulation and filtering, to yield separate hinge and swivel error outputs as d-c voltages.

2.7.1.10 Polarity Switch Drive - The Polarity Switch Drive is a four-transistor amplifier, to provide gain to the output of a photo-voltaic silicon diode. The photodiode is activated by a pin-light bulb, and turned off by a code wheel interrupting the light beam.

Each time the scan crosses the optical axis, or rosette center, the Polarity Switch Drive actuates the Polarity Switch to invert the trailing edge of the signal pulse.

2.7.1.11 Channel Selector Drive - The Channel Selector Drive is an amplifier driven in a fashion identical to the Polarity Switch Drive. This photodiode output is amplified by the Channel Selector Drive and used to drive a pair of mechanical synchroverter switches which determine the channel frame reference.

2.7.1.12 Acquisition Motor Drive - The Acquisition Motor Drive circuit controls the acquisition motor, depending on the presence or absence of planet pulses at the output of the fixed slicing level circuit. When the acquisition motor is turned on, the rosette scan pattern is rotated at a rate of 1/4 rpm in a search mode. This circuit also turns on the acquisition motor if the sun is scanned by the scanner.

2.7.1.13 Altitude Circuit - The duty cycle of the planet signal pulse train, at the output of the fixed slicing level-clipper, is a function of the distance from the planet. This circuit yields a d-c output proportional to the pulse width of the signal and hence is a function of altitude.

2.7.1.14 Planet Intensity - The amplitude of the planet pulses, at the output of the preamplifier (before limiting), are a measure of the intensity of the received radiation. This circuit yields a d-c output proportional to the peak amplitude of the signal and hence it is a planet intensity indicator, or crude radiometer.

2.7.1.15 Regulated ± 15 v Power Supply - This circuit converts 50v, 2400 cps square wave input power to regulated ± 15 volts d-c, to provide circuit power in non-critical areas.

2.7.1.16 Preamplifier Power Supply - Using the same input power as the ± 15 v regulated supply, this circuit feeds regulated +20 volts to the preamplifier and Solar Presence Circuits and regulated and highly filtered ± 20 v excitation to the bolometer bridge. This supply, or "super-regulator," provides the isolation necessary for handling low level signals.

2.7.2 Circuit Operation

2.7.2.1 The Infrared Detector/Bolometer (See Figure 2-6) - The detector consists of two thermistor elements connected in a bridge circuit. One arm is the active flake which receives the incoming radiation; the other arm is a temperature compensating flake of similar characteristics which is shielded from external radiation. The two flakes are oppositely biased at ± 20 v, and their junction is connected to the parallel inputs of the preamplifier and solar presence circuits.

Radiation impinging upon the active flake will change its temperature and therefore its resistance. The voltage at the junction will change accordingly.

2.7.2.2 Preamplifier (See Figure 2-6) - When a target warmer than its background is detected by the scanner, positive going signal pulses are coupled to the base of Q1 (on circuit board A5A1A2) through C4 (of the same board). These signal pulses are amplified by the first four stages and then coupled to an emitter follower output stage Q2 (on circuit board A5A1A1). A portion of this output signal, a positive voltage, is fed back to the emitter of A5A1A2 Q1 where it tends to buck the positive signals applied to the base, reducing the input current to the stage and increasing the input impedance of the amplifier.

In order to limit the slope of the top of the detector pulse to less than 5% "droop" (to better define the level at which the pulse is later sliced), a low frequency cut-off of 0.1 cps was selected. The root mean square value of the fluctuation in the instant of pulse slicing is proportional to RMS system noise and inversely proportional to the slope of the pulse around the slicing level.

As system noise is an increasing function — and the inverse slope a decreasing function — of the bandwidth of the preamplifier, the existence of an optimum bandwidth is indicated. If the pulse is sliced at mid-height, the bandwidth requirement would be around 200 cps. As the slicing level of this instrument

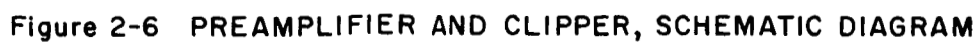


Figure 2-6 PREAMPLIFIER AND CLIPPER, SCHEMATIC DIAGRAM

is fixed and as the signal intensity cannot be predicted with precision, the slicing may occur at widely varying relative pulse heights. It was therefore decided to use a greater bandwidth than optimum, of about 700 cps, in order not to degrade system performance if slicing occurs off the ideal mid-height of the pulse. The increase in slicing instant fluctuations with mid-height slicing and greater bandwidth is estimated to be 50% above the optimum.

A series low pass filter, at the output of the preamplifier, tends to offset the increase in uncertainty introduced by the greater bandwidth.

2.7.2.3 Solar Presence Circuit (See Figure 2-6) - The solar presence circuit consists of a three-stage transistor feedback amplifier, with an overall gain of 18, feeding a regenerative two-stage amplifier. The input to this circuit is in parallel with that of the preamplifier, yielding a combined input impedance of about 600K ohms. The two transistor amplifier, Q1 and Q2 of A5A1A4, operates in a regenerative mode. Q1 is normally cut off, but saturates when pulsed with amplitudes exceeding 120 mv, turning off Q2 which is normally saturated. On the falling edge of the pulse, Q1 cuts off again, and with the help of Q2 going toward saturation, a steep positive going pulse is sent to the emitter of Q1 (on A5A1A2), blocking the preamplifier for a period of about 40 milliseconds. To energize this circuit, a strong pulse, such as obtained when scanning the sun, is required.

2.7.2.4 Fixed Slicing Level — Amplifier Clipper (See Figure 2-6) - Preamplifier output is fed through the complementary emitter follower A5, Q5-Q6, buffer stage to the positive clamp formed by C1-Q4. The signal pulses are clamped to 8.7 volt, determined by the +15v supply and 6.3v zener diode CR1. The clamping transistor A5Q4 is driven from A5Q3 of the differential amplifier.

The clamped signal is fed through emitter follower A5Q1 to the input transistor A5Q2 of the differential amplifier. An adjustable d-c potential is fed to A5Q3, the other side of the differential amplifier. The signal side of the differential amplifier is normally saturated at +10v. When the clamped input pulse exceeds the d-c potential fed into the base of A5Q3, the input transistor A5Q2 cuts off and the potential on the collector of this stage falls to -10 volts.

The sliced output of ± 10 v is taken from the collector of A5Q2 and fed through the complementary emitter follower A5, Q7-Q8 to the double anode zener diode A5 CR3, to be clipped at ± 6 v. The sliced and clipped signal is then fed to the positive and negative clamp and polarity switch for further processing.

2.7.2.5 Positive and Negative Clamp and Polarity Switch (See Figure 2-7) - Negative Channel - Negative clamping is performed by A3, C1-CR1. The clamped signal is fed through the cascaded emitter followers A3Q1 and A3Q2 to zener diode A3 CR2 to be clipped at -6.3v.

Positive Channel - Zener diode A3 CR4 carries the current determined by the constant current source A3Q6. The voltage developed across A3 CR4 is

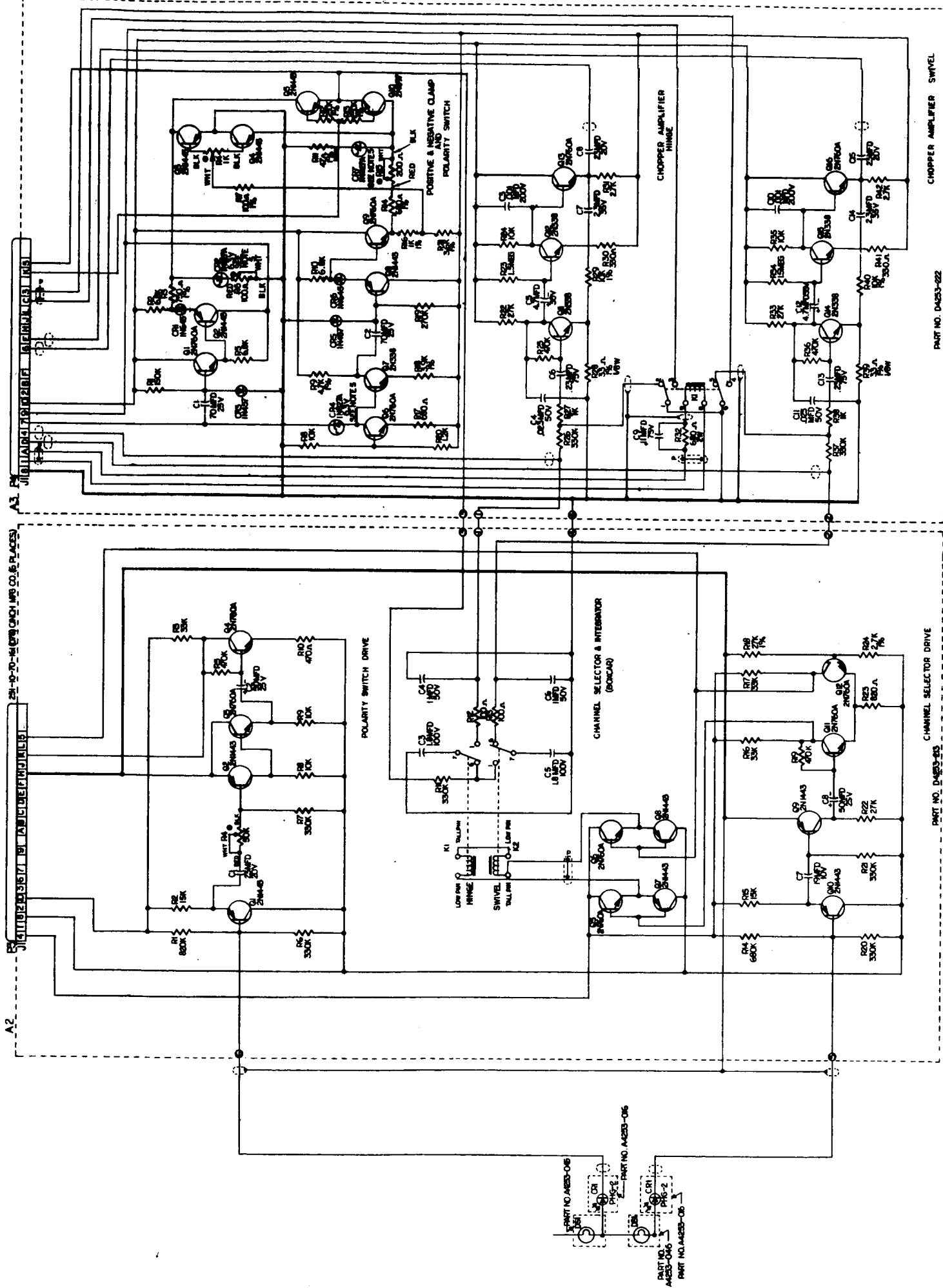


Figure 2-7 POLARITY SWITCH, CHANNEL SELECTOR AND CHOPPER AMPLIFIER SCHEMATIC DIAGRAM

inserted in series with the signal to bring it to the correct level for handling by the inverter A3Q7. The inverted signal is clamped positively by A3 C2-CR5 and then fed through the cascaded emitter followers A3 Q8 and A3 Q9 to A3 CR7 where it is clipped at +6.3v.

The switch A3 Q3-Q4 shorts both channel outputs in the absence of a signal pulse to yield a low level output within ± 5 millivolts of ground. When a signal pulse appears, A3 Q3-Q4 opens for the duration of the pulse. Potentiometer A3R4 balances A3 Q3-Q4 to reduce d-c offset. Diodes A3 CR1, A3 CR6 and potentiometer A3R15 are for temperature compensation. A3R6 is adjusted to adjust the negative channel pulse heights to the positive channel pulse heights.

The polarity switch is actuated by its own driver amplifier at the instant the instruments field of view coincides with the optical axis. At this instant the center terminal is switched from the positive to the negative channel or vice versa, depending on which scan lobe the axis crossover occurs.

2.7.2.6 Channel Selector and Integrator (Box Car) (See Figure 2-7) - The output of the polarity switch is connected through an integrating resistor A3R11 alternately to the integrating capacitors A3C3 and A3C5 by means of two single pole double throw syncroverter switches. The alternation separates the intelligence relating to one orthogonal axis from the other. The charge accumulated on A3C3 during one integration period is a measure of the unresolved hinge deviation while the charge accumulated on A3C5 is a measure of the unresolved swivel deviation.

Each integration period is bisected by a change of state of the polarity switch. When the planet is ideally centered in the rosette scan, each signal pulse is bisected by this change of state. Positive and negative inputs of equal amplitudes and duration are fed in sequence to the integrating capacitors producing zero net change at the end of the integrating period.

When the axis of the sensor does not coincide with that of the planets local vertical, the signal pulse for one or both channels is not bisected symmetrically by the change of state of the polarity switch. As the positive and negative clamp is adjusted to yield a constant amplitude signal output, the only change is in the symmetry of the pulse relative to the polarity switch. This assymetry shows up as a net change on the integrating capacitor at the end of the integration period.

At the instant when A3C3 begins its integration period, A3C5 has completed its own and is connected by the synchronous switch A3K2 through the surge limiting resistor A3R13 to the holding capacitor A3C6 sharing its charge with the latter capacitor. This charge is a measure of the swivel deviation and is fed to the swivel chopper amplifier.

Similar analysis describes the operation of the hinge integrator.

2.7.2.7 Chopper Amplifiers (See Figure 2-7) - The d-c voltages at the output of the box car, corresponding to unresolved hinge and swivel deviations, are chopped at the two modulator contacts of the double pole-double throw mechanical chopper A3K1 at a 400 cps rate and amplified, to be fed into and mixed by the synchro resolver. The three transistor a-c amplifiers used have a gain of 300 and an input resistance of 50K ohms.

To prevent too rapid discharge of the holding capacitors A2C4 and A2C6 of the box car, the chopping is buffered by A3R26 in the hinge, and A3R37 in the swivel channel. These same resistors and the input resistance of the a-c amplifiers form voltage dividers. The d-c to peak-to-peak conversion gain from box car to the primary of the synchro resolver is 50.

2.7.2.8 Synchro Resolver (See Figure 2-8) - The primary of the synchro resolver is geared 1:1 with the mechanical acquisition head. Information from the 400 cps choppers is fed into two windings with axes at 90° on the primary (rotor) of the resolver. The axes of the two secondary (stator) windings of the resolver are also at 90° with each other.

In the acquisition mode the rosette scan pattern is rotated about the axis of the sensor. The primary of the resolver is also rotated the same number of degrees about its own axis. As the rosette scan changes angular position in space, the original off-axis error, if any, detected by the scanner becomes a trigonometric function of the angular deviation. The same applies to the resolver.

By coupling the rotation of the resolver primary with that of the rosette scan pattern, the secondary of the resolver will yield an output which is constant for a fixed off-axis error, no matter what the angular difference is between the platform and rosette axes. The output of the resolver is fed to the 400 cps demodulators.

2.7.2.9 400 CPS Demodulator (See Figure 2-9) - The two secondary windings of the synchro resolver; one winding carrying hinge error information, and the other swivel error information, are each fed to single stage amplifiers, A4Q7 for hinge, A4Q9 for swivel. The output of the amplifiers feed emitter follower stages A4Q8 and A4Q10.

The a-c signals present at the emitters of A4Q8 and A4Q10 are synchronously demodulated by a second set of contacts of the same mechanical chopper A3K1 which modulated the d-c outputs of the box car circuit. Demodulation occurs by synchronously clamping the signals to ground to yield half-wave rectification. A4C11 and A4C17 are the clamping capacitors, A4R22 and A4R30 are current limiting resistors. The clamped signals are filtered by A4R23, C19, C21 for hinge and A4R31, C18, C20 for swivel.

The output filter capacitors A4C19, C21, C18 and C20 are polar capacitors connected back-to-back for outputs of both polarities. The a-c voltage gain between the secondary of the resolver and the emitter follower is about 15.

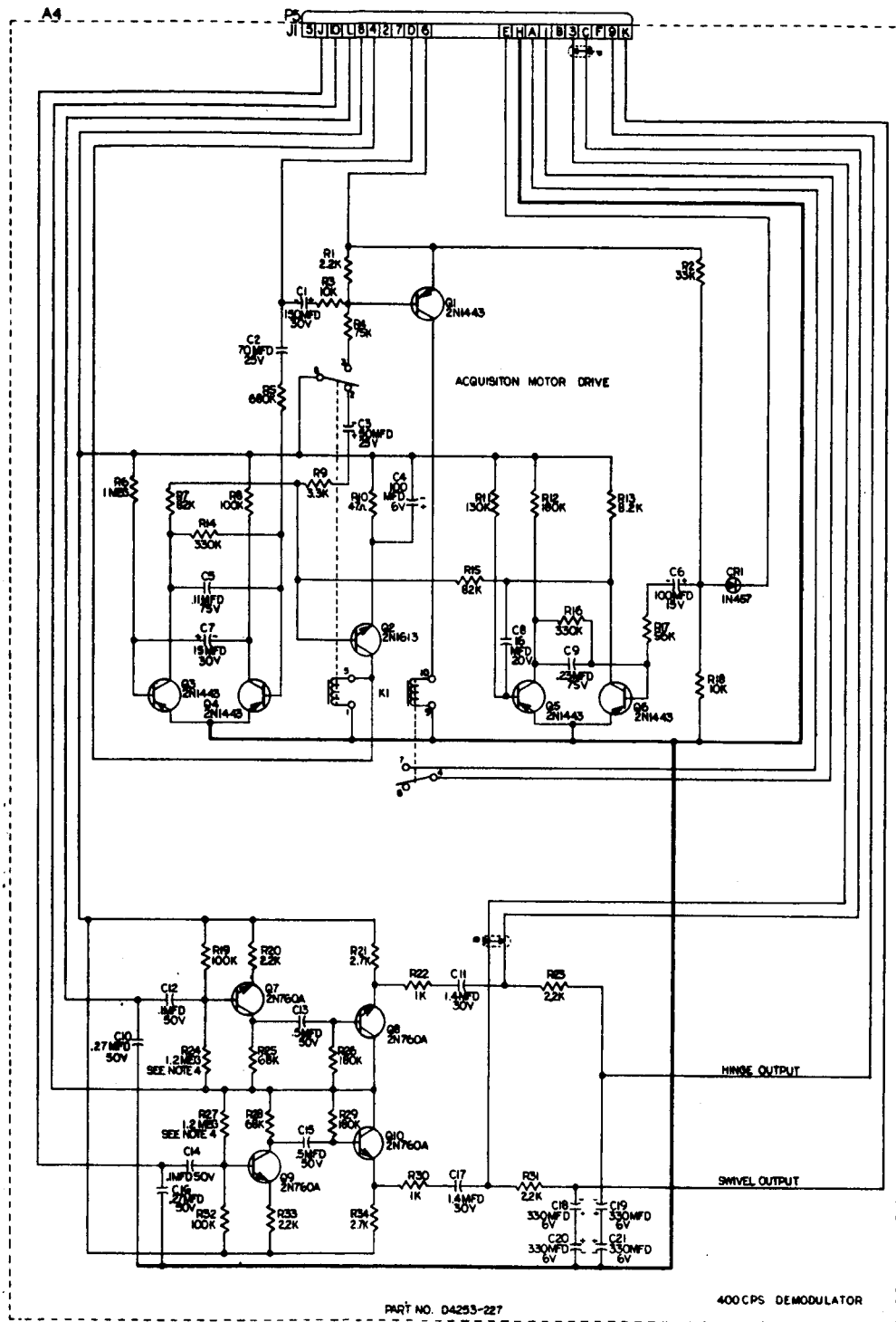


Figure 2-9 ACQUISITION DRIVE, SCHEMATIC DIAGRAM

2.7.2.10 Polarity Switch Drive (See Figure 2-7) - The output of the photodiode is fed through emitter follower buffer stage A2Q1 to the common emitter stage A2Q2. In order to steepen the sides of the output pulse A2Q2 is driven into saturation and cutoff by the input wave with its linear region of operation corresponding to a fraction of the rising and falling edges of the input pulse. A2R4, the series base resistor to A2Q2 allows for adjustment of the level at which the slice is taken from the input pulse. This adjustment is used to minimize hinge-swivel crosstalk as a function of synchro resolver rotor position inaccuracy. In effect, it slightly alters the point where the change of state of the polarity switch occurs.

A2Q3 is another emitter follower buffer stage. A2Q4 further reduces the width of the slice taken from the input wave, to produce a pulse of very steep sides. The output of this circuit drives the single pole-double throw polarity switch.

2.7.2.11 Channel Selector Drive (See Figure 2-7) - The output of the photodiode is fed through emitter follower A2Q10 to the common emitter stage Q9. This stage is overdriven to steepen the rising and falling slopes of the input wave. The output of A2Q10 feeds the common emitter differential pair A2Q11 and A2Q12, which are also overdriven to further increase the slope of the edges of the input pulse.

The differential pair has balanced outputs which drive the balanced complementary symmetry emitter followers A2Q5-Q7 and A2Q6-Q8. The outputs of the complementary emitter pairs are fed to the driving coils of the two syncroverters A2K1 and A2K2 of the channel selector and integrator circuit to supply a channel frame reference.

2.7.2.12 Acquisition Motor Drive (See Figure 2-9) - There are two input paths to the circuit; the junction of A4C1-C2, fed by the amplifier clipper, and diode A4CR1, fed by the output of the preamplifier. In the absence of planet signals monostable multivibrator A4Q3-Q4 is in a stable state with A4Q4 saturated. With A4Q3 saturated, the base-emitter junction of A4Q4 is forward biased and Q4Q2 acts like a closed switch. Current through this transistor energizes coil 5-1 of latching relay A4K1 which closes contacts 4 and 7. This completes the 400 cps circuit for acquisition motor A1B3, turning it on. Current flow also closes contacts 8-3 of A4K1 providing bias to A4Q1. Some current flows through coil 10-9 of A4K1, but not enough to overcome the holding current in coil 5-1.

If a planet pulse is received, the negative going output of the clipper circuit (junction of A5Q7-Q8 emitter) is applied to the base of A4Q4 turning it on, which turns off A4Q3. As A4Q3 turns off, its collector becomes more negative and turns off A4Q2. This removes holding current from contacts 5-1 of A4K1.

At the same time, a negative pulse is sent to A4Q1 which now drives enough current through coil 10-9 to change the state of the relay. Contacts 7-4 open to disable the acquisition motor. Current through coil 10-9 also open

contacts 8-3 and close contacts 8-2 which remove bias from A4Q1 and cuts off this stage. This removes current from coil 10-4 yielding the controlling function to coil 5-1 and therefore to Q2. As long as signal pulses are received, A4Q3 tends to remain cutoff thus preventing A4Q2 from going into conduction and switching the latching relay to the other mode.

If the circuit stops receiving planet pulses, A4Q4 does not turn on and A4Q3 saturates-returning forward bias to A4Q2 energizing coil 5-1. This closes contacts 7 and 4, which returns 400 cps power to the acquisition motor and introduces rotation of the planet scan. Contact 8-2 is also opened and 8-3 closed by this action.

In order to prevent erratic jogging of the acquisition motor in the period between a momentary turnoff of A4Q4 and the arrival of the next planet pulse, the contacts 8-2 complete an R-C path to introduce a time lag in the base circuit of Q2, preventing relay chatter.

In the other mode of operation, if the sun is scanned the output of the preamplifier is sent negatively toward ground for about 40 milliseconds by the solar presence circuit. This makes the normally reversed biased diode A4CR1 of the acquisition motor drive conduct, turning on monostable multivibrator A4Q5-Q6. Transistor A4Q5 turns off and transistor A4Q6 saturates, forward biasing A4Q2 energizing coil 5-1 of the latching relay. This closes contacts 4 and 7 completing the 400 cps circuit for the acquisition motor, turning it on. Current flow through A4Q2 also closes contacts 8-3 of A4Q1 providing bias to that stage. Some current flows through coil 10-9 but not enough to overcome the holding current in coil 5-1.

The acquisition motor keeps turning until the sun pulse disappears and a planet pulse arrives to stop it, in the manner described earlier.

2.7.2.13 Altitude Circuit (See Figure 2-10) - The input to this circuit is fed from the fixed slicing level-amplifier clipper circuit, in a form of a pulse train. A6C4 and A6CR4 clamp the signal negatively to about -2v set up by diodes A6 CR6, CR7 and CR8. These diodes compensate for the temperature characteristics of A4CR4 and the emitter follower output stage. The clamped signal is fed through the low-pass filter A6R8-C5, leaving only the d-c component of the clamped signal to drive the output emitter follower A6Q3.

Diode A6CR5 provides the base current path for A6Q3 under no-signal conditions, preventing the output of the circuit from going positive. The circuit output is kept "definite negative" under all input conditions so that a circuit malfunction, resulting in zero volts output could not be erroneous interpreted as an indication of planet distance.

Series resistor A6R7 protects the circuit from overload due to an accidental short circuit at the output.

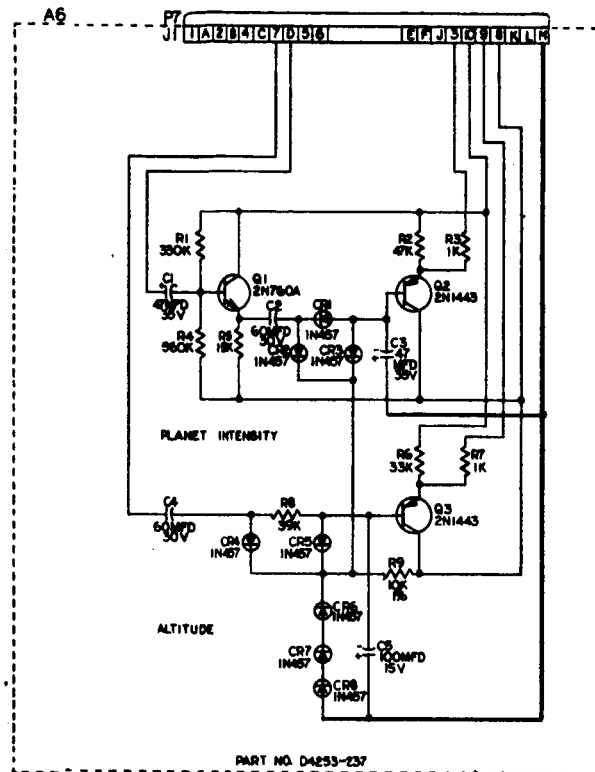


Figure 2-10 PLANET INTENSITY AND ALTITUDE CIRCUITS, SCHEMATIC DIAGRAM

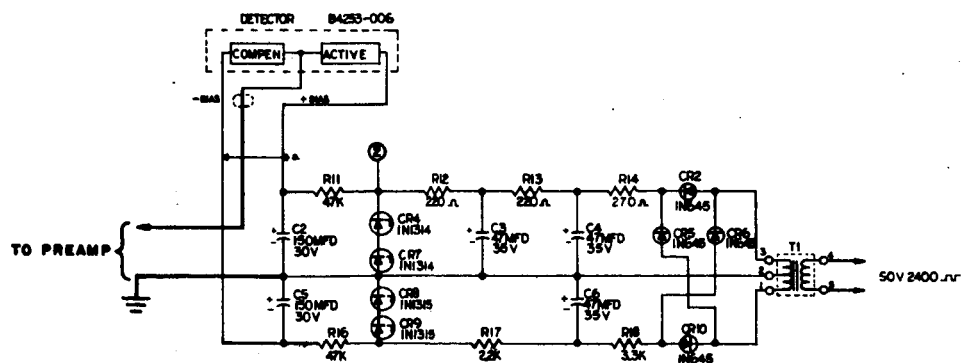


Figure 2-11 PREAMPLIFIER POWER SUPPLY, SCHEMATIC DIAGRAM

2.7.2.14 Planet Intensity (See Figure 2-10) - The input emitter follower, A6Q1, prevents the circuit from loading the preamplifier and feeds the preamplifier output to the negative clamp A6C2-CR2, of -2v, set up by the same diodes referred to in the previous section (altitude circuit). A6CR1-C3 form a peak detector and drive the emitter follower output stage A6Q2. A6CR3 provides a base current path for the no-signal condition, keeping the output negative under all conditions in the same manner that A6CR5 performs the function for the altitude circuit.

Series resistor A6R3 protects the circuit from overload due to an accidental short circuit at the output.

2.7.2.15 Preamplifier Power Supply (See Figure 2-11) - Power supplied to this circuit is a 50 volt, 2400 cps square wave. The small input transformer A5T1 and full wave rectifiers A5CR2-CR5 and A5CR6-CR10 provide unregulated positive and negative d-c voltages. The filters A5R14-C4, A5R13-C3 and the zener diodes A5CR4-CR7 provide filtering and regulation for the ± 20 volt requirements of the preamplifier.

Resistor R11 and capacitor C2 provide further filtering to the positive bolometer bias voltage. A5R18-C6, the zeners A5CR8 and A5CR9, A5R17 and A5R16-C5 regulate and filter the negative bolometer bias.

Resistors A5R11 and A5R16 also serve as current limiters in series with the thermistor bridge as safeguards for operation in high ambient temperatures.

2.7.2.16 Regulated ± 15 Volt Power Supply (See Figure 2-12) - The 50v, 2400 cps square wave input power is fed to transformer A7T1. The center tapped secondary of A7T1 feeds two full wave bridge rectifiers; A7CR1-CR3 for the negative output and A7CR2-CR4 for the positive output. The unregulated d-c passes through series transistor regulators.

For the positive supply, the parallel transistors A7Q1 and A7Q2 form the series element of the regulator. A7Q4 and the emitter follower A7Q3 provide feedback from the output to govern the series element. Zener diode A7CR7 provides the reference voltage for the feedback loop while a voltage proportional to the output is taken at the junction of A7R6 and A7CR5.

Diode A7CR5 provides temperature compensation while A7R3, A7C2 and zener diode A7CR6 pre-filter and pre-regulate the reference voltage. Resistors A7R1 and A7R2 help equalize the power dissipation in transistor A7Q1 and A7Q2.

The large amount of feedback present in the series regulator serves to hold the output impedance at low frequency to a very low value of about 0.2 ohms. Output voltage variation is about $\pm 0.5\%$ for an input variation of $\pm 7\%$ and is nominally set at +15 volts.

Similar remarks and circuit description apply to the negative voltage regulator.

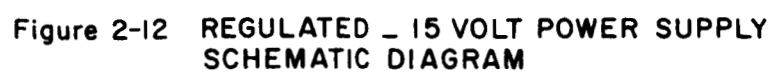


Figure 2-12 REGULATED - 15 VOLT POWER SUPPLY SCHEMATIC DIAGRAM

Section 3.0 SCANNER CONSTRUCTION

3.1 STRUCTURE

Design effort was made to keep the center of gravity close to the mounting plane, therefore the heavy mechanical elements are all located in this area. The major mechanical parts are relatively massive, to provide support and rigidity necessary for the precision gears and bearings. From a structural standpoint the major mechanical parts are considerably over-designed.

The scanner is mounted by three "ears" located 90° apart on a 7-1/4 inch bolt circle (JPL Drawing No. D4800734, Horizon Scanner, Assembly, Mars Configuration, Control Drawing). The electronic circuit boards are cantilevered on three support posts, anchored to the gearplate, which, in turn, is located between the mounting ears, see Figures 3-1 and 3-2.

The use of stress skin construction, borrowed from aircraft design techniques, plays an important role in maintaining a rigid, yet lightweight structure. Instead of using massive support posts to achieve strength and rigidity, the exterior skin, or can, is used as the load bearing member. Since the circuit board stack represents a cantilevered load for lateral (perpendicular to optical axis) forces, the three slim posts securing the circuit boards act merely as spacers, or check rods, with negligible contribution. For axial forces, however, these posts are fully utilized as load members while the exterior skin makes no contribution.

Each round circuit board is 1/16 inch thick and is laminated to a 1/16 inch thick magnesium "subchassis". This subchassis is a spinning having a 3/8 inch lip around the periphery. The 3/8 inch wide lip has an outside diameter which slip-fits inside the exterior cover. Thus the round circuit boards are effectively supported by the external "can" or cover.

A calculation of the bending stiffness of the exterior 6-1/2 inch diameter by 0.032 thick cylindrical can shows a factor of 4500:1 when compared to the combined bending stiffness of the three 0.281 inch diameter support posts. Stated in another fashion, the three support posts would have to be 2-1/4 inches diameter in order to have a rigidity equal to the thin wall exterior can. It is apparent that a stress skin construction achieves great economies in weight and size, that would not have been possible with more conventional design.

3.2 TEMPERATURE CONTROL

Under normal operating conditions, the Horizon Sensor consumes 7-1/2 watts of electrical power; during the acquisition mode when the second motor is operating, total power consumption approaches 10 watts. In the vicinity of Venus, the absorbed solar energy is nearly twice that near Earth. The heat from these two sources must be dissipated in the only way possible — by radiation to the space background. Since the energy radiated into space is dependent on

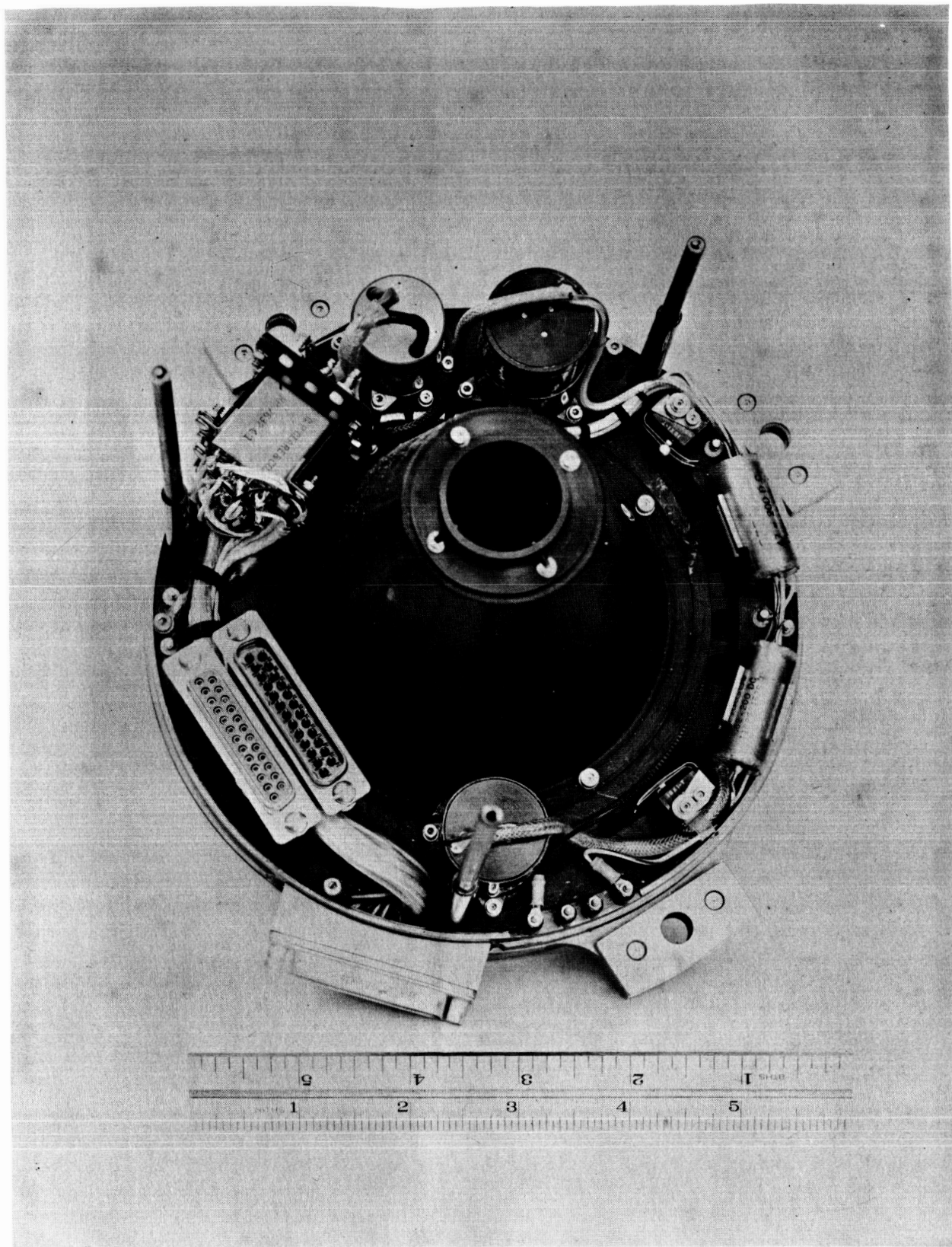


FIGURE 3-1 GEAR PLATE ASSEMBLY: CIRCUIT BOARD A1

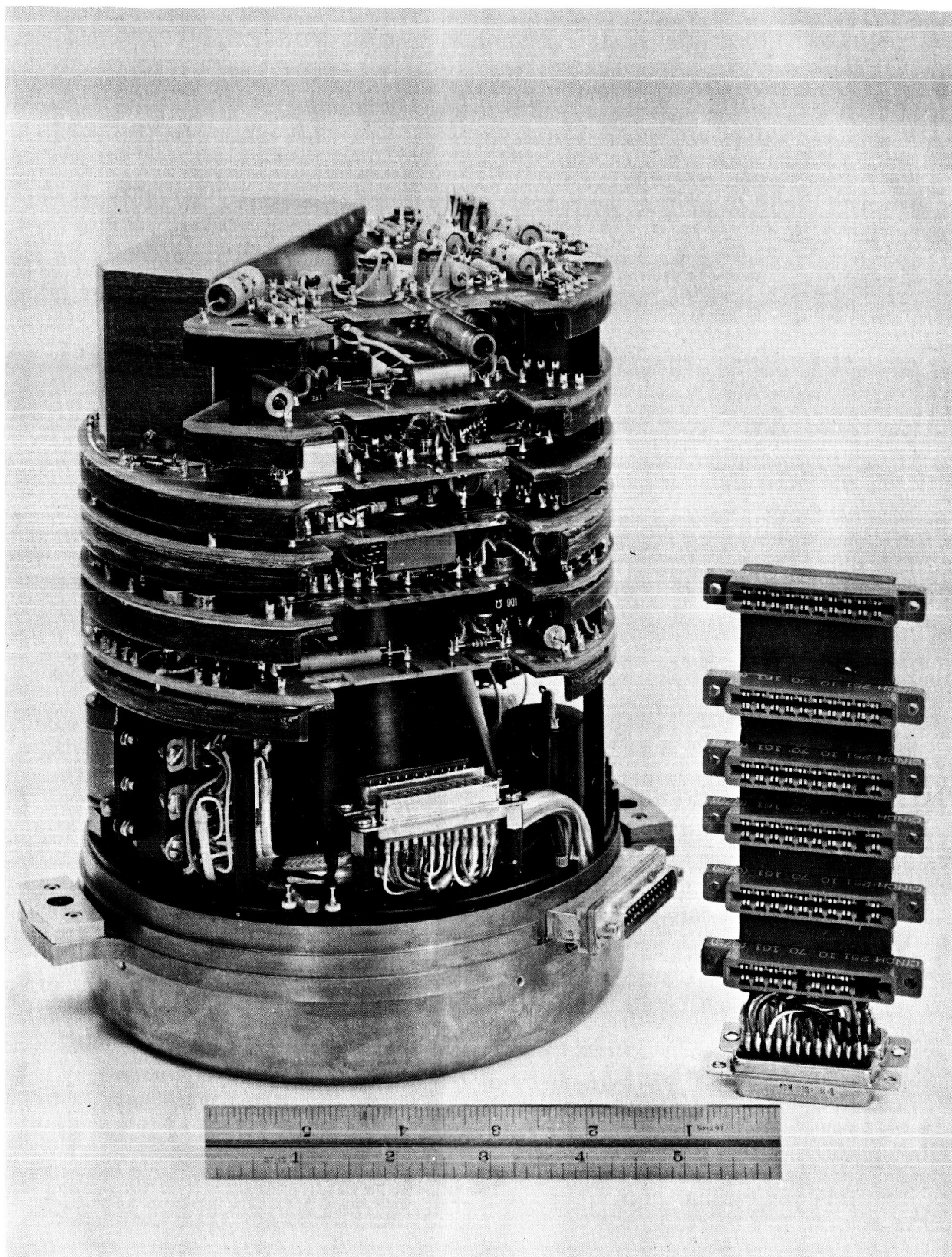


FIGURE 3-2 HORIZON SCANNER ELECTRONICS ASSEMBLY

the fourth power of the instrument temperature, means have been sought to maintain this temperature within the tolerable limits imposed by the thermistor bolometer detector: -40°F to $+175^{\circ}\text{F}$.

The aluminum window cover, together with the spun aluminum case, present a relatively uniform appearance, and have simple geometry. Calculations show that passive temperature control, using special coatings applied to the outer surfaces of the Horizon Sensor, will adequately maintain temperature. Active controls, such as shutter elements, are therefore not necessary.

The $4\text{-}3/4$ inch diameter germanium window, however, posed a special problem. Radiation below 1.8 microns, where the bulk of the sun's energy exists, is largely absorbed by the germanium window, imposing a severe heat load on the equipment. An aluminum cover or shutter is used over the window during the in-operative period. Upon planet approach, explosive squibs retract a pin, allowing a spring loaded hinge to open the cover for operation. The "mouse trap" style springs which open the cover also act as hinge points. This circumvents the use of moving parts in a hard vacuum. An exterior latch is also provided to ensure that the cover, when open, is safely latched, and does not obscure optics.

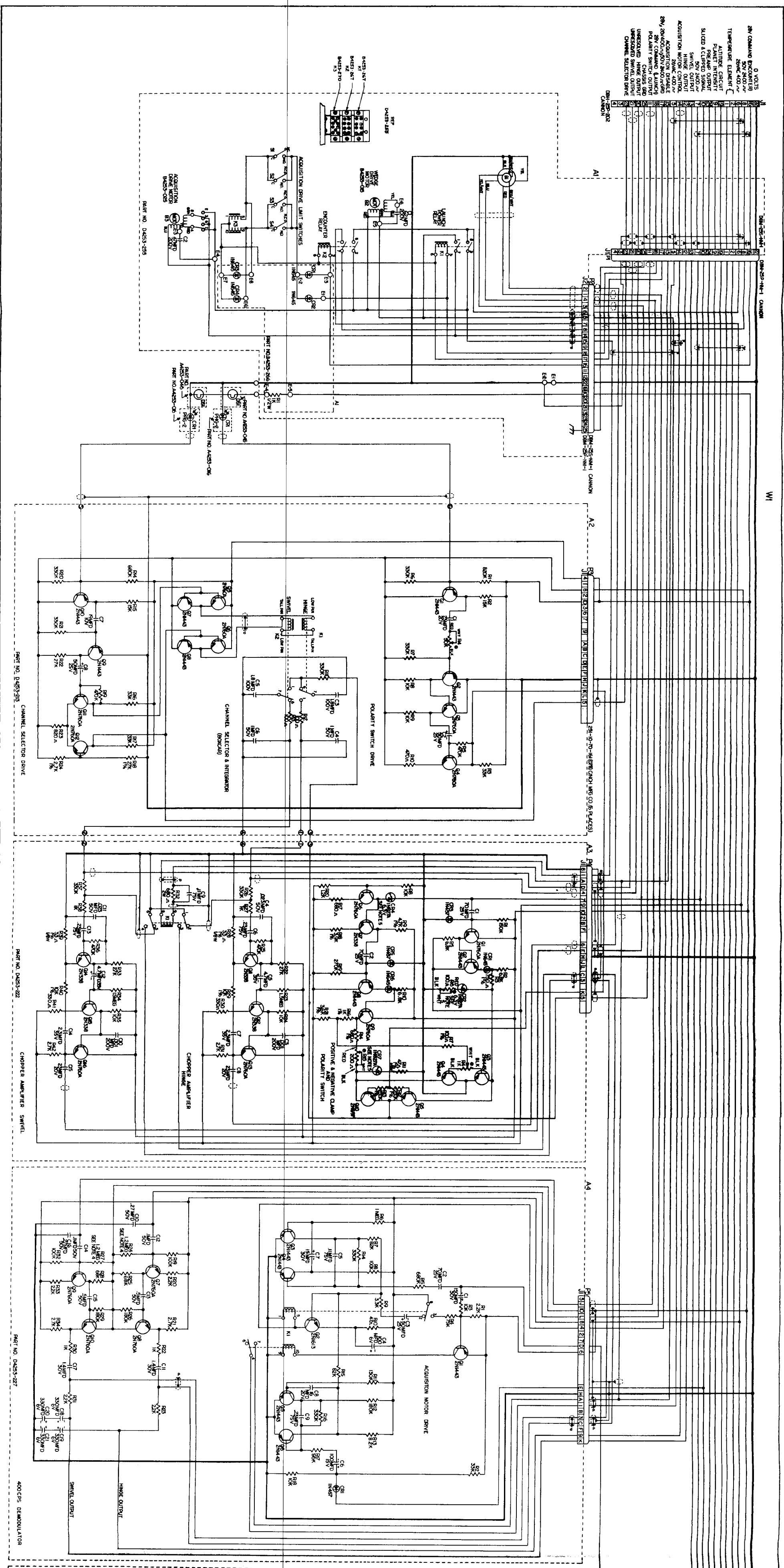
In addition to its temperature control function, the window cover also safeguards the detector. During operation, the small duty cycle of a $3/4^{\circ}$ sun target will not cause any damage, but with stationary prisms a fixed sun image may appear in such a position as to burn the detector. Hence the window is covered until the unit is turned on.

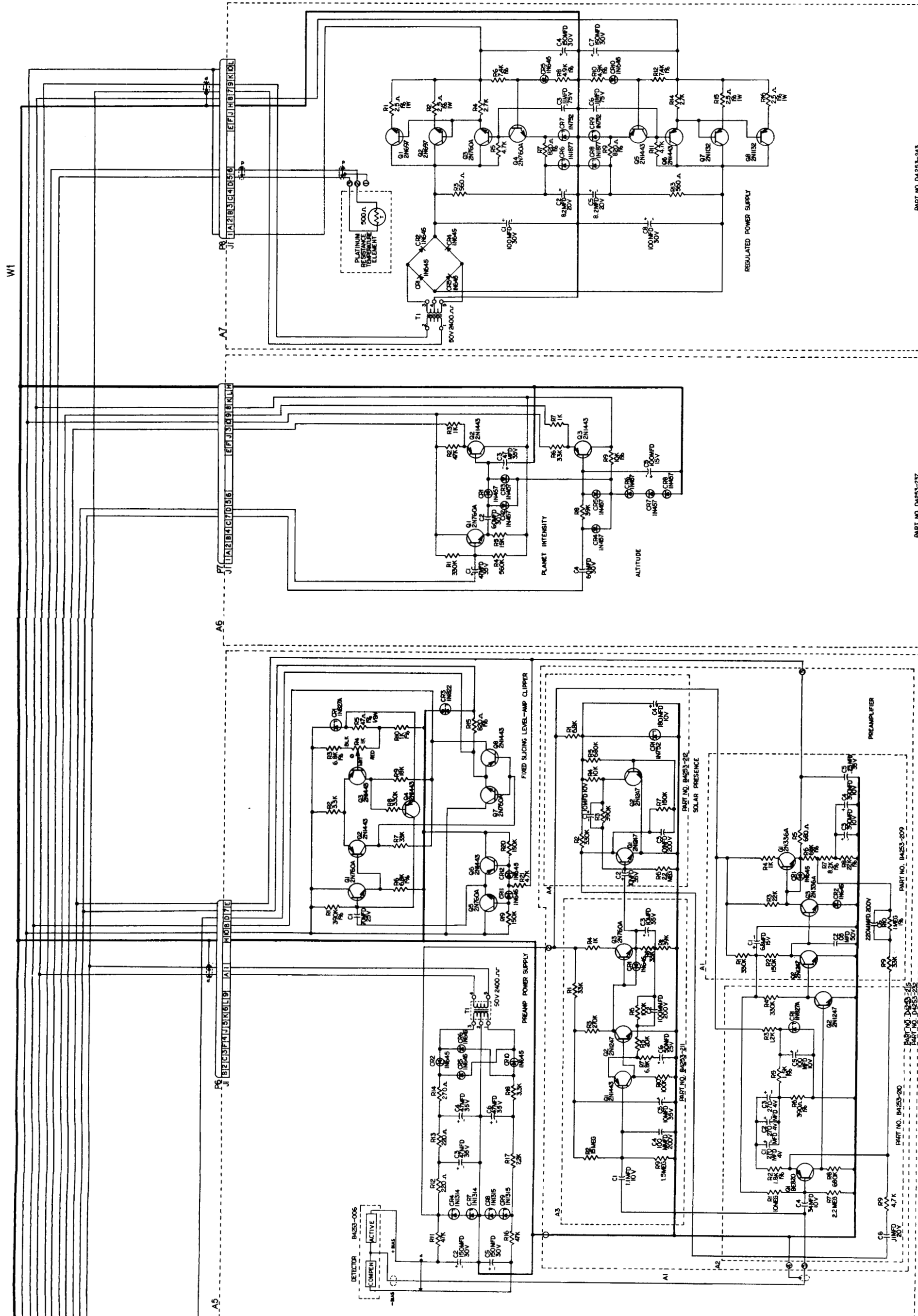
To check on effectiveness of temperature control during the mission, a 500 ohm platinum resistance element was attached to the thermistor bolometer. The temperature of the bolometer, which is the critical element in the Horizon Sensor, is telemetered back to Earth.

3.3 THE HERMETIC SEAL

To maintain a known environment, and to avoid the difficulties of designing a drive mechanism for operation in hard vacuum, the sensor is hermetically sealed. The filling medium is a mixture of 90% nitrogen, 10% helium, with a dew point of -72°F , at a pressure of 1 pound gage (16 psia).

Early in the program considerable effort was spent on developing solder seals. The aluminum front and rear covers were plated with electroless nickel to facilitate the soldering. Experiments were also made with various aluminum solders. None of these efforts proved practical, and there was serious concern of possible heat damage. Epoxy was found to provide an excellent seal, and eliminated the possible damage to expensive germanium optical elements due to excess heating, thermal shock, or differential expansion. The epoxy chosen is Hysol No. 4326 with No. 3421 hardener, which provides good adhesion, and is slightly resilient, or non-brittle. The latter property is important, since the epoxy seals are load bearing, and are subject to shock and vibration.





NOTES:

1. REFERENCE DESIGNATIONS ARE ABBREVIATED. PREFIX THE DESIGNATION WITH THE UNIT NUMBER OR ASSY DESIGNATION OR BOTH
2. ALL RESISTORS VARY ±10% UNLESS OTHERWISE SPECIFIED
3. ALL CAPACITORS NON-POLARIZED UNLESS OTHERWISE SHOWN
4. R04 & R27 SHALL BE SELECTED NOMINAL VALUE 12MΩ
5. RANGE 750KΩ TO 1.6MΩ MAX (ASSY #4)
6. CR2, CR4 & CR7 SHALL BE 5.0MΩ ± 5% (ASSY #3)

REFERENCE DRAWINGS
84253-259 LIST FORM WIRING DIAGRAM

[illegible]

The sealing operation was accomplished through a filling tube of 1/4 inch diameter copper. After all epoxy seals were cured, the entire unit was immersed in water and bubble checked using dry nitrogen at 10-15 psi internal pressure. The absence of bubbles indicated that no leaks greater than 25 micron-cubic feet per hour were present. The filling tube was next coupled to a Veeco MA-9 mass spectrometer, and the unit evacuated. Helium was "squirted" around the seals, using a small rubber hose. If there were no gross indications of leaks, the unit was flushed and back filled for three cycles. The copper tube was pinched off at 1 pound positive pressure, and a bead of solder put on the end.

Gross internal volume of the system is approximately 315 cubic inches while net internal volume is assumed to be 200 cubic inches. Assuming a linear leak rate to provide a conservative estimate, and assuming a loss of no more than 50% of the gas content in a six month mission, the maximum allowable leak rate has been calculated to be 100 cubic inches per six months or 10^{-4} -std. cc/sec.

The above calculation is conservative because progressive loss of pressure provides less driving force to the leak. The actual decay of pressure is an exponential function. Thus the leak rate, as measured in a bell jar with a mass spectrometer, is a rate based on the maximum available differential pressure. Experience with several units showed measured leaks were several orders of magnitude less than that allowed.

3.4 ASSEMBLY TECHNIQUE

3.4.1 Assembly of Electronics

The electronics are mounted on six stacked circular printed circuit boards and a base plate. The base plate is actually the gear plate for the wedge drive motors. Bifurcated terminals are used extensively on the six circular electronics boards for greater reliability and ease of fabrication. Cabling is run perpendicular to, and on one side of, the stacked boards. Inter-board electrical connections are made by connectors placed along the cable length. This method enables the external circuit wiring to be minimum in length and decreases the possibility of pickup loops. To minimize noise pickup in the low level outputs of the channel selector integrators, they are wired directly to the input of the chopper amplifier circuits.

3.4.2 Assembly of Germanium Window

Germanium has a thermal coefficient of $3.3 \times 10^{-6}/^{\circ}\text{C}$ vs. aluminum at $13 \times 10^{-6}/^{\circ}\text{C}$. When bonding the germanium window into the aluminum bezel, or front cover, the joint is cured at 60°C , the maximum operating temperature specified for the Horizon Scanner. In this way, the aluminum bezel is expanded to its maximum limit, as is the germanium window. When the epoxy is cured at this temperature, it fills the space between the window and the bezel without being subjected to any stress. As the assembly is cooled, after curing, the aluminum

bezel contracts to a greater degree than the germanium window, thus subjecting the epoxy joint to compressive forces.

As epoxy is far more tolerant of compressive stress than tensile or shear stress, the bonding resin is thus being used to maximum advantage. Furthermore, the joint is not dependent on the bond strength of the epoxy.

If the assembly were cured at a lower temperature, expansion of the aluminum relative to the germanium may cause bond failure. Indeed, this technique is used to remove a bonded window from the aluminum bezel by baking at 180°C. At this temperature the bond separates, and the window is easily freed from the bezel.

A similar technique is used to bond the front and rear covers to the steel center section. Again the aluminum housings have a greater coefficient of expansion than the steel center section, allowing the 60°C bonding technique to be used to advantage.

3.5 GEARS AND BEARINGS

All prism drive gears are 72 pitch, 20° pressure angle, AGMA Precision Class I. Since the drives are uni-directional, backlash is not of particular concern.

The synchro resolver gear and mating pinion are 96 pitch. The gears contained in the acquisition gear head are 120 pitch. All other gears in the acquisition drives are 72 pitch.

A single thin-cross section, large diameter bearing (torque tube bearing) is used to support the acquisition assembly. This bearing is a four point contact design, and is preloaded to prevent free play.

The two prisms are arch supported by a single large thin bearing, which is also a four point contact type. These bearings are selected for low torque in order to conserve motor power.

All other bearings are the miniature type, ABEC-7 class.

3.6 LUBRICATION

In the event of pressure loss, provision has been made for vacuum operation of bearings. CBS dry film lubricant, together with conventional bearing oil, are used as the bearing lubricant. The dry film alone has a tendency to stick and gall. This is believed to be caused by contaminants, or foreign particles, entering the bearings during testing. The addition of lubricating oil does not deteriorate the dry film, and seems to inhibit the destructive action of foreign particles.

Pressure loss would cause evaporation of the lubricating oil, leaving the dry film material. Even contaminated, the dry film has an operating life of 100 to 150 hours, which is adequate margin for 10 hours of operation at planet encounter.

3.7 SCAN AND ACQUISITION DRIVE MOTORS

The prism drive motor has operating characteristics uniquely suited to this application. Developed and manufactured by BEC, these 8 pole induction motors have a no-load speed of 7800 rpm, and a maximum power point at 7200 rpm. In addition to a high efficiency of 50%, the motor is exceptionally smooth running and free of "wow". This property is especially important when working with pulse position detection techniques, since scan speed variation would cause an apparent shift in time of the pulse edge.

Speed regulation per second is not so important as the smooth running, or uniform velocity requirement. Long term speed variations will not cause deteriorated performance of the instrument.

The acquisition drive is powered by a 400 cycle, size 11 induction motor. The motor is similar in construction to the drive motor used for the prisms, but requires only 1-1/2 watts of power. A gear head with a ratio of 1803:1 is attached to the motor. The output pinion of the gear head is meshed directly to the integral gear on the acquisition ring.

3.8 STRETCH CORDS

As the acquisition section rotates through 90°, the lamps and photodiodes used to generate sync signals also rotate. To bring power to the lamps, and to carry signals from the photodiodes, electrical connections must be maintained while this section rotates. To avoid the use of slip rings, and their attendant problems in the event of pressure loss, insulated electrically conductive elastic stretch cords are used. These cords act as a stretchable umbilical cable, and are laid over a portion of the acquisition ring. The amount of stretch is 100%, and the rated life under these conditions is 25,000 cycles.

3.9 THE USE OF BERYLLIUM IN SCANNER S/N 104

In the early design of the Horizon Sensor, the major mechanical parts were constructed from SAE 52100 steel, in order to match thermal coefficients of the thin ring bearing supporting the prisms, and the acquisition assembly.

Delicate magnetometer experiments would be upset by these steel parts, and so a study was made of substitute materials. A Study Report, BEC-4253-R22A "Non-Magnetic Structural Materials for Venus and Mars Horizon Sensor" concluded that beryllium offered an ideal replacement, having a thermal coefficient closely matched to the bearing, and also being a lightweight, strong material.

One unit, Serial No. 104, was made from the beryllium and was approximately 2 pounds lighter than other units.

The use of beryllium created a problem of gear material selection. The prism housings, and acquisition ring both have integral gear teeth. Made of SAE 52100 steel, these integral gears offer excellent wear properties. Converting these steel parts to beryllium creates a serious hazard; small wear particles may be generated by beryllium gears, which could be toxic to personnel. Furthermore, the properties of beryllium gears are unknown, leading to doubts regarding their use.

Delrin was selected as a replacement material, and a life test was performed. A Test Report, "Delrin Gear Life Test for Venus and Mars Horizon Sensor" concluded that after 2000 hours operating life, the Delrin gears showed no sign of deterioration. Serial No. 104 unit was constructed with delrin gears and operated satisfactorily.

Section 4.0 TEST EQUIPMENT, PROCEDURES AND RESULTS4.1 SIMULATION OF TARGETS

The simulation of the planets must be based upon the spectral characteristics of their self-emitted radiation, which are functions of their surface temperatures (or in the case of Venus, the temperature at the top of its atmosphere). Theoretically, at least, perfect simulation may be obtained by utilizing a hemisphere or disk which is heated (or cooled) to the temperature of the planet against a background of absolute zero. Practically, the temperature-controlled hemisphere or disk may be set against a background of a more realizable higher temperature corresponding to liquid nitrogen with very small error. Due to the fact that the energy gradient is proportional to the difference of the fourth powers of the two temperatures, it is apparent that utilizing a background which is one-half the absolute temperature of the simulated planet would yield an error of only 6%.

Carrying this concept a little further, we can state the equation which applies and examine it for its implication:

$$\Delta E = k (\zeta_1(\lambda) T_1^4 - \zeta_2(\lambda) T_2^4),$$

where

- ΔE = energy gradient between target and background (w/cm^2)
- k = constant of proportionality
- T_1 = temperature of target ($^{\circ}\text{K}$)
- T_2 = temperature of background ($^{\circ}\text{K}$)
- $\zeta_a(\lambda)$ = spectral passband characteristic constant for the optical system at a specific blackbody temperature (T_a)

Any judicious combination of "planet" and background temperatures may be selected to yield the same ΔE which would result when T_1 is taken as the actual temperature of the planet and T_2 is the temperature of background space. A series of curves are shown in Figure 4-1 for the various temperatures of Venus and Mars shown in Table I. These curves are based upon representative composite spectral characteristic of the optical elements in the sensor and for anti-reflection coatings which are peaked at 12.5 microns. For "rough and ready" simulation, an idealized spectral passband is often assumed in a manner similar to designating the passband of amplifiers (i.e., the -3 db points). A more accurate method is that of calculating the integrated product of the composite optical transmission curve and each blackbody curve.

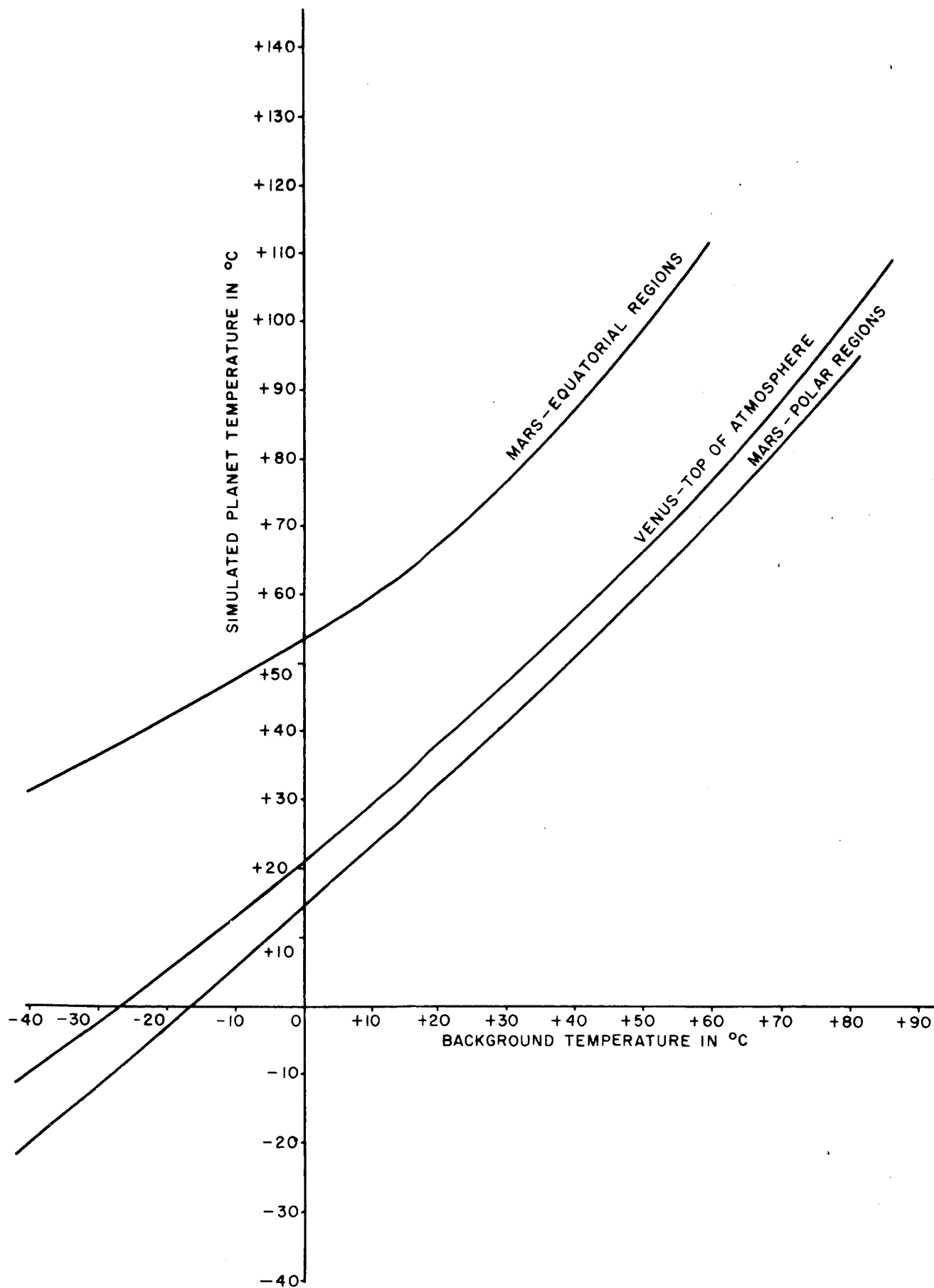


Figure 4-1 PLANET SIMULATOR TEMPERATURES

TABLE I. PERTINENT PARAMETERS OF VENUS AND MARS
FOR THEIR INFRARED DETECTION

Parameter	Venus		Mars	
	Surface	Top of Atmosphere	Equator	Pole
Distance from Sun (Relative to Earth = 1.0)	0.723		1.524	
Temperature ($^{\circ}\text{K}$)	430	225	280	205
Peak Wavelength of Radiant Energy Emitted	7μ	13μ	10μ	14μ
Total Radiant Energy ($\text{W-cm}^{-2}\text{-Sr}^{-1}$)	0.063	0.0046	0.011	0.0032
Percentage Energy Tying In Spectral Interval 1.8 - 18 microns	85	49	64	42.5

4.2 TEST EQUIPMENT

4.2.1 Target

A large flat aluminum plate, coated with an electrically resistive surface layer, is used to simulate the planet energy. An autotransformer is used to control the power applied to the resistive film, and the surface temperature is monitored by thermocouples. Zapon black paint is applied on top of the electric film to achieve an emissivity of 0.9.

In front of the heated plate, an extended mask, or baffle, with a center hole is mounted. The back of the mask is insulated to prevent heating, and is spaced forward approximately 4 inches to allow free circulation of air between the mask and heated plate.

The diameter of the center hole in the mask, and the distance at which the horizon scanner is located, establish the subtended angle of the target. To the scanner, the center hole appears as a luminous disc situated against an "ambient" background. As a rule of thumb, an object located more than 40 focal lengths away is essentially at "infinity" with respect to the optical system. Since the effective focal length of the Horizon Scanner is only $3/4$ inch, a target distance of 15 feet is more than adequate to simulate a planet without resorting to corrective optical elements.

4.2.2 Rotary Turntables

To complete the test setup, the Horizon Scanner is mounted on rotary turntables. Although a single turntable will suffice, a two-axis setup containing two perpendicular turntables offers more convenience. In this way, it is not necessary to turn the Horizon Scanner 90° to test each orthogonal axis.

The center of rotation of both turntables is designed to coincide with a nodal point of the optics, to avoid translation errors.

The transfer function of the scanner may be measured for both linearity and scale factor by rotating the turntable controlling the hinge or swivel axis.

An 18 power telescope is attached to the scanner mounting fixture to provide a visual indication of the pointing direction of the turntables. Another 18 power telescope can be set into the scanner mounting fixture to check perpendicularity of the surface against which the scanner is mounted, and also to check the parallax of the other telescope.

4.2.3 The Test Console

A BEC fabricated test console is used for electrical checkout of the Horizon Scanner. The console contains all power supplies, test junctions and selector switches. Panel meters display 400 cycle voltage and current, as well as 2400 cycle voltage and current. A recording ammeter monitors 400 cycle motor current. A dual trace, long persistence oscilloscope is situated convenient to the test junctions. A running time meter is coupled to the 400 cycle power switch, to record running time of the mechanical elements.

Prominently displayed are two large voltmeters; one for hinge output and one for swivel. These zero-centered meters are calibrated both in terms of angle ($\pm 0.5^\circ$ full scale) and voltage (± 3 vdc full scale).

4.3 TEST PROCEDURES AND RESULTS

The Horizon Scanner is mounted in a holding fixture attached to the two rotary turntables. The target is heated to a temperature of 35°F above ambient, which is equivalent to a 230°K planet against space background. After connecting the test console to the Horizon Scanner, the tests are conducted in accordance with JPL Specification 30856. A typical data sheet and results of the Performance Evaluation Tests for Horizon Scanner Serial No. 103 is reproduced at the end of this section. The comments which follow apply equally to all the above tests.

Operation with targets as large as 52° proved difficult without using external optical elements, as they had to be impractically large when placed sufficiently far from the sensor to be in focus. Testing was therefore confined

to subtended angles of no more than 16° . Furthermore, during the tests, a crosstalk between hinge and swivel channels was observed, occurring when the acquisition drive was in operation. As the hinge and swivel axes of the scanner are rotated in space, the synchro resolver performs a coordinate transformation of hinge and swivel information, in order to take into account any angular difference between the rotating rosette pattern and the auxiliary platform axes (which are fixed). Any small fixed errors within either signal channel will progressively transfer over to the other channel as the synchro resolver rotates. Only by laborious tuning and aligning can the two channels be so closely matched that crosstalk is held within the specified limits of $\pm 0.025^\circ$.

DATA SHEET

PERFORMANCE EVALUATION TESTS

Horizon Scanner Serial No. 103

Total operating hours of horizon scanner for tests 28.5

Notes: 1. All tests performed with power shall be as follows:

- 2400 cps 50 ± 1% volts rms, square wave
- 400 cps 26 ± 2% volts rms
- DC 28 ± 2% volts

2. Tests indicated with an asterisk to be repeated with 2400 cps power set @ 48.5 ± 1%, 51.5 ± 1%

Test No.	Test Parameter	Test Conditions	Nominal Test Value & Tolerance	Measured Test Value	Test Performed By & Date
1.	400 cps current	a) Scan motor only operating b) Scan & acquisition motor (26±0.2 volts, rms 400 cps applied power)	210 max.	<u>200 mV</u>	<u>DHC 5/9/63</u>
2.	28-volt dc power	a) 28 volts dc applied to pin 16 b) 28 volts dc applied to pin 18	280 max.	<u>278</u>	<u>DHC 5/9/63</u>
3. *	2400 cps power	28 volts dc to pin 18 50 volts rms 2400 cps square wave to pin 7 and 8	max. max.	<u>28 V</u> <u>28 V</u>	<u>DHC 5/9/63</u> <u>DHC 5/9/63</u>
4. *	Sensitivity & signal level	Measured at preamp output pin 24. Ratio peak signal to rms noise. 35.0 ± 0.5 °F temperature gradient between simulated planet and room temperature background (equivalent to 230 °K planet against space background)	53.5 watts 46.5 100 min.	50.0v <u>4.55</u> 51.5v <u>4.95</u> 48.5v <u>4.25</u> 50.0v <u>105</u> 58.5v <u>105</u> 51.5v <u>107</u>	<u>DHC 5/9/63</u> <u>DHC 5/9/63</u> <u>DHC 5/9/63</u> <u>DHC 5/9/63</u> <u>DHC 5/9/63</u> <u>DHC 5/9/63</u>
	Peak signal level	3.1 ± 0.3 volts	50.0v	<u>3.4 V</u>	<u>DHC 5/9/63</u>
			<u>46.5</u>	<u>3.4</u>	<u>DHC 5/9/63</u>
			<u>53.5</u>	<u>3.4</u>	<u>DHC 5/9/63</u>

DATA SHEET

PERFORMANCE EVALUATION TESTS

Test No.	Test Parameter	Test Conditions	Nominal Test Value & Tolerance	Measured Test Value	Test Performed By & Date
5.	Noise	Measured at hinge and swivel outputs. Pins 12 and 13			
	a)	Scanner masked to see homogeneous background with no simulated planet; scanner rotated through full acquisition cycle.	Peak noise voltage and bias offset not greater than ± 0.15 volts	HINGE $\pm 10V$ SWIVEL $\pm 1.09V$	DHC 5/9/63
	b)	Scanner nulled for ± 0.01 volts dc on hinge and swivel against following size planets at $35.0 \pm 0.2^\circ F$. T temperature gradient.			
		Scanner then rotated through full acquisition cycle. Peak noise voltage and bias not greater than:			
		4°	± 0.15 volts	HINGE $\pm 2V$ SWIVEL $\pm 0.27V$	DHC 5/9/63
		16°	± 0.15 volts		
		40°	± 0.30 volts		

DATA SHEET PERFORMANCE EVALUATION TESTS

JPL Spec. No. 30856 A

Test No.	Test Parameter	Test Conditions	Nominal Test Value & Tolerance	Measured Test Value	Test Performed By & Date
6. *	Scale factor, polarity and saturation level	Measured at angular displacement from electrical null			
a) 4° planet Angular Error					
Hinge	Swivel	Hinge	Swivel	Hinge	Swivel
+0.1°	0°	+0.6 ±0.1 v dc	0 ±0.15 v dc	+0.6V	+0.02V
*+0.2°	0°	+1.2 ±0.2 v dc	0 ±0.2 v dc	50.0 v ±1.3V	+1.06V
				46.5 48.5 v ±1.3V	+0.05V
				53.5 51.5 v ±1.3V	+1.060V
+1.0°	0°	+2.0 v dc min.	0 ±0.3 v dc	+4.6V	+1.70V
-0.2°	0°	-1.2 ±0.2 v dc	0 ±0.2 v dc	-1.2V	-1.2V
-1.0°	0°	-2.0 v dc max.	0 ±0.3 v dc	-4.9V	-1.0V
0°	+0.1°	0 ±0.15 v dc	+0.6 ±0.15 v dc	0.0V	+1.6V
*0°	+0.2°	0 ±0.2 v dc	+1.2 ±0.2	50.0 v ±1.08V	+1.13V
				53.5 51.5 v ±1.08V	+1.13V
				46.5 48.5 v ±1.05V	+1.13V
0°	+1.0°	0 ±0.3 v dc	+2.0 v dc min.	-1.35V	+4.7V
0°	-0.2°	0 ±0.2 v dc	-1.2 ±0.2 v dc	+1.18V	-1.3V
0°	-1.0°	0 ±0.3 v dc	-2.0 v dc max.	+1.70V	-4.5V

DHC 5/9/63
DHC 5/9/63
DHC 5/9/63
DHC 5/9/63
DHC 5/9/63
DHC 5/9/63
DHC 5/9/63
DHC 5/9/63
DHC 5/9/63
DHC 5/9/63
DHC 5/9/63
DHC 5/9/63
DHC 5/9/63
DHC 5/9/63
DHC 5/9/63

DATA SHEET

PERFORMANCE EVALUATION TESTS

Test No.	Test Parameter	Test Conditions	Nominal Test Value & Tolerance	Measured Test Value	Test Performed By & Date
6.	(cont'd)				
		<u>Hinge</u> <u>Swivel</u>	<u>Hinge</u> <u>Swivel</u>	<u>Hinge</u> <u>Swivel</u>	
		b) 40° planet			
		+0.2° 0°	+1.45 ± 0.2 v dc 0 ± 0.2 v dc		
		-0.2° 0°	-1.45 ± 0.2 v dc 0 ± 0.2 v dc		
		0° +0.2°	0 ± 0.2 v dc +1.45 ± 0.2 v dc		
		0° -0.2°	0 ± 0.2 v dc -1.45 ± 0.2 v dc		
7. *	Acquisition mode	a) Scanner masked for period of 5 minutes	Acquisition motor operates continuously	50.0 v 0.1K 51.5 v 0.1K 48.5 v 0.1K	DHC 5/9/63 DHC 5/9/63 DHC 5/9/63
		b) Scanner unmasked while operating in acquisition mode with 2° planet in field of view, and at following angular displacements from scanner axis			
		0°	Scanner acquisition motor stops within 1 minute time maximum and remains in track mode		
		8°			
		16°			
8. *	Solar Discrimination	(Test conditions and test values to be specified)		O.K. ALL TESTS	DHC 5/9/63

DATA SHEET

PERFORMANCE EVALUATION TESTS

Test No.	Test Parameter	Test Conditions	Nominal Test Value & Tolerance	Measured Test Value	Test Performed By & Date
9. *	Boresight Alignment	Horizon scanner boresighted on 16" diameter planet simulator, at distance of at least 20' and operated at $35.0 \pm 1.0^\circ\text{F}$ temperature rise above ambient background, so that angular error between normal to surface defined by horizon scanner mounting pads and simulated planet is $0 \pm 0.025^\circ$			
		Acquisition motor operated continuously			
		Hinge	53.5° 46.5° $0 \pm 0.300 \text{ v dc}$	$50.0 \text{ v} \pm .3 \text{ V}$ $51.5 \text{ v} \pm .28 \text{ V}$ $48.5 \text{ v} \pm .28 \text{ V}$ $50.0 \text{ v} \pm .3 \text{ V}$	DHC 5/9/63 DHC 5/9/63 DHC 5/9/63 DHC 5/9/63
		Swivel	53.5° 46.5° $0 \pm 0.300 \text{ v dc}$	$51.5 \text{ v} \pm .31 \text{ V}$ $48.5 \text{ v} \pm .31 \text{ V}$	DHC 5/9/63 DHC 5/9/63
10.	Leak Test	Horizon scanner placed in Bell jar and leak rate tested with mass spectrometer (90% N_2 and 10% H_2 gas at 15 psig)			
		Maximum H_2 leak rate	std cc/hr	0.0185 cc/hr	RFE 5/9/63

Section 5.0 CONCLUSIONS AND RECOMMENDATIONS

This highly developed, highly specialized Horizon Scanner probably represents the ultimate among mechanically driven Horizon Scanners. Recent advances in the development of "no moving parts" horizon scanners (containing electronically scanned thermopile detector arrays), however, have brought their accuracy and resolution close to that of the mechanical scanners. This new type of scanner has greater reliability and much longer operating life.

Despite impending obsolescence, the tracking performance of this instrument has yet to be surpassed, and represents a notable achievement in the art of horizon scanners. With the latter in mind, the following recommendations are tendered.

1. The ZnS anti-reflection coating applied to the optics should be optimized to achieve maximum transmission at minimum signal levels. This occurs when viewing a 200°K target, whose peak transmission occurs at 14.5μ . Therefore, to maximize signal from this lowest temperature target, the anti-reflection coating should be changed to peak at 14.5μ , instead of the present 12.5μ .

2. The operation of the Horizon Scanner can be greatly simplified by eliminating the acquisition drive. The Horizon Scanner can be left in a continuous "search" mode without deterioration of performance. This is accomplished by gearing the prisms so that the gear ratio is not exactly an integer. For example, a gear ratio of 2.99:1 or 3.01:1 will produce a four leaf rosette scan which slowly and continually "crawls" or precesses. Thus the scan pattern slowly revolves in space, remaining in a perpetual acquisition mode.

This change will eliminate the acquisition drive motor, and all attendant relays and circuitry. Also, the signal presence and solar presence circuits will become simplified. The feasibility of this mode of continuous operation of acquisition has been demonstrated in dynamic tracking tests at JPL. The manual control was used on the acquisition motor so that the rosette scan pattern continued to rotate during the entire tracking test. Although an off-axis target takes longer to acquire, there is no other degeneration of performance. Small off-axis targets are acquired in a series of "steps". As the scan rotates, it alternately acquires and loses the target, and then reacquires as the next scan lobe intersects. Finally, when the target approaches optical center, it is continuously scanned, and there are no further scan discontinuities. The only penalty incurred is additional gearing required to drive the synchro resolver at the appropriate speed. A slight change is required in generating sync pulses; part of the new gear drive to the synchro can be used to drive the reference wheel at the proper speed to generate sync pulses. On the other hand, the reliability would be improved through reduction of components and, therefore, a reduction in power, weight and size.

3. Sun lying close to the scan will produce errors (see Sources of Errors). A sun detector, or sun shield should be added (as well as long wavelength pass filters) to overcome this source of error. A circular detector surrounding the primary detector flake could be used to warn against sun presence, or cause momentary disabling. An aluminum mask can be incorporated in the image plane of the detector to minimize local heating. Other means, such as a dichroic mirror placed in front of the detector and operating a sun detector placed off-axis, could also be used.

Alternately, the use of a long wavelength pass filter would decrease the magnitude of sun-induced errors. An 8μ cut-on filter, for example, will reduce the relative sun intensity by a factor of 50. The use of even longer wavelength filters, such as a 12μ cut-on filter, not only reduces the effect of the sun, but also reduces the effect of temperature variations on opposite horizons.

4. Emergency provision should be added for start-up in the event that the prism drive motor fails to start during the terminal phase of the mission. This may take the form of applying a surge voltage to the motor, or an additional set of starting windings to augment the low starting torque of the motor. Other possible devices are mechanical release springs, or explosive squibs.

APPENDIX A

ROSETTE VELOCITY ANALYSIS

In polar coordinates, the expression for a four leaf rosette is

$$r = a \cos 2\theta$$

If $\theta = \omega t$ and the expression is solved for the tangential velocity of the detector image projected on a fixed plane perpendicular to the optical axis of the scanner, then

$$\vec{v} = \frac{ds}{dt} = \sqrt{\left(\frac{d\theta}{dt}\right)^2 + \left(\frac{dr}{dt}\right)^2}$$

solving for v , the expression becomes

$$\vec{v} = \frac{\alpha\omega}{2} [10 - 6 \cos 4\omega t]^{1/2}$$

where ω = angular velocity of the slow prism, in radians per second

α = angular displacement of each rosette leaf tip, from the optical axes, or 35°

for \vec{v}_{\max} , $\cos 4\omega t$ must equal -1 , or

$$\vec{v}_{\max} = 2\alpha\omega = 2(35^\circ)(11) = 770^\circ/\text{sec.}$$

for \vec{v}_{\min} , $\cos 4\omega t$ must equal $+1$, or

$$\vec{v}_{\min} = \alpha\omega = 35^\circ(11) = 385^\circ/\text{sec.}$$